#### ROVIBRATIONALLY-RESOLVED PHOTODISSOCIATION OF HD

by

#### CLAUDIA E. NICULAS

(Under the Direction of Phillip C. Stancil)

#### **ABSTRACT**

The photodissociation of most molecules is typically obtained through pre-computed, exponentially-attenuated fitted photo rates, whose assumptions are likely to describe few astronomical environments. Furthermore, calculations of cross sections for the photodissociation of the isotopomer of molecular hydrogen, HD, are currently available only for the J=0 levels of the ground electronic state. Explicit calculations of cross sections from all rovibrational states are necessary in order to compute HD photo-destruction rates for any environment and radiation field. To this end, we have directly calculated the partial cross sections for the Lyman and Werner transitions of HD from all 400 rovibrational levels of the ground electronic state into the continua of the upper electronic states. This required input of potential curves and dipole transition moments derived by standard ab initio techniques. The partial cross sections were calculated for a number of wavelengths ranging from 100 Å to the dissociation threshold from each rovibrational state.

INDEX WORDS:

HD, Rovibrational energies, Photodissociation, Cross sections, Lyman transition, Werner transition, Potential energy curves, Dipole transition moments, Photo-destruction rates

## ROVIBRATIONALLY-RESOLVED PHOTODISSOCIATION OF HD

by

CLAUDIA E. NICULAS

B.S., University of Georgia, 2006

A Thesis Submitted to the Graduate Faculty of the University of Georgia in Partial Fulfillment of the Requirement for the Degree

MASTER OF SCIENCE

ATHENS, GEORGIA

2008

© 2008

Claudia E. Niculas

All Rights Reserved

## ROVIBRATIONALLY-RESOLVED PHOTODISSOCIATION OF HD

by

## CLAUDIA E. NICULAS

Major Professor: Phillip C. Stancil

Committee: Robin L. Shelton

Susanne Ullrich

Electronic Version Approved:

Maureen Grasso Dean of the Graduate School The University of Georgia August 2008

# **DEDICATION**

I dedicate this thesis to my parents, Nicolae and Elvira Niculas, my late grandfather, Ioan Dancu, as well as to my good friends Oana Leventi-Perez, Sonia Ahluwalia, and Judith Norton.

#### **ACKNOWLEDGMENTS**

I would like to thank, above all, my advisor, Phillip C. Stancil, for his invaluable help and support throughout this work. I further thank the members of my committee, Robin Shelton and Susanne Ullrich, Christopher Gay and the entire Stancil research group, Steven Lewis, Craig Wiegert, and the overall Physics and Astronomy department. Most especially, I thank Loris Magnani, for his advice and support throughout the years, and my friends and colleagues Wesam El-Qadi and Mohua Bhattacharya. Last but not least, I would like to acknowledge Theodore Shifrin from the Mathematics department, for his significant impact throughout my academic career.

# TABLE OF CONTENTS

			Page
ACKNOWL	EDGEMENTS		v
LIST OF FIG	GURES		vii
CHAPTER			
1	INTRODUC	TION	1
2	ROVIBRATIONAL ENERGIES OF HD		3
	2.1	Theory	3
	2.2	Calculation and Results	8
3	PHOTODISSOCIATION OF HD.		13
	3.1	Theory	13
	3.2	Calculation and Results	16
4	CONCLUSION AND FUTURE TOPICS.		35
	4.1	Summary	35
	4.2	Future Work	36
REFERENCI	E <b>S</b>		38
APPENDIX:	Rovibrational	Energies of the Ground State of HD	39

# LIST OF FIGURES

	Page
Figure 2.1: <i>B</i> and <i>C</i> Potential Energy Curves.	3
Figure 2.2: Illustration of Rovibrational Energy Levels Within an Electronic State	5
Figure 2.3: Ground ( <i>X</i> ) State Potential Energy Curve.	9
Figure 2.4: <i>X</i> State Rovibrational Energies by Corresponding <i>v</i>	10
Figure 2.5: X State Rovibrational Energies by Corresponding J.	11
Figure 3.1: Lyman ( $B \leftarrow X$ ) Dipole Transition Moment	18
Figure 3.2: Werner ( $C \leftarrow X$ ) Dipole Transition Moment.	19
Figure 3.3: Example of Vibrational ( <i>X</i> ) and Continuum ( <i>C</i> ) Wavefunctions	20
Figure 3.4: Lyman Transition Cross Sections for $v = 0$ and several $J$	22
Figure 3.5: Werner Transition Cross Sections for $v = 0$ and several $J$	23
Figure 3.6: Lyman Transition Cross Sections for $v = 9$ and several $J$	24
Figure 3.7: Werner Transition Cross Sections for $v = 9$ and several $J$	25
Figure 3.8: Lyman Transition Cross Sections for $J = 0$ and several $v$	26
Figure 3.9: Werner Transition Cross Sections for $J = 0$ and several $v$	27
Figure 3.10: Lyman Transition Cross Sections for $J = 9$ and several $v$	28
Figure 3.11: Werner Transition Cross Sections for $J = 9$ and several $v$	29
Figure 3.12: Lyman Transition Allison & Dalgarno Comparison and HD vs H <sub>2</sub>	30
Figure 3.13: Werner Transition Allison & Dalgarno Comparison and HD vs H <sub>2</sub>	31
Figure 3.14: Lyman Transition Comparison between HD and H <sub>2</sub>	32
Figure 3.15: Werner Transition Comparison between HD and H <sub>2</sub>	33
Figure 3.16: Lyman / Werner and HD / H <sub>2</sub> Comparison	34

#### Chapter 1

#### INTRODUCTION

The HD molecule contains an ordinary Hydrogen atom as well as a Deuterium atom whose nucleus consists of both a proton and a neutron. It is one of many molecules contained in a variety of astronomical objects whose origins, evolution, and dynamics are active research fields. In particular, the soon-to-be launched Herschel Space Observatory will render possible the exploration of the sub-millimeter to far infrared portion of the electromagnetic spectrum with unprecedented sensitivity and resolution. This will provide insight into such astronomical environments as starburst and ultraluminous infrared galaxies, photon-dominated regions, protoplanetary disks surrounding young stars, various interstellar clouds, and circumstellar environments. To maximize such insight, modeling of the relevant formation and destruction processes is required. This allows for the determination of species abundances, which in turn helps one interpret spectral lines such as those observable with Herschel ( $\lambda = 60 - 670 \mu m$ ), including those due to HD.

Photodissociation of relevant species, via calculating the cross sections for various product channels, is one component of such modeling of formation and destruction processes. To calculate the cross sections for a diatomic molecule, it is first necessary to compute the rovibrational energies, i.e. the energies due to vibration of the two atoms and rotation of the molecule as a whole, corresponding to the ground electronic state. Once cross sections are obtained, one can calculate the photo-destruction rates of a particular molecule and for a particular environment by integrating the cross sections over the local radiation field. Currently, the photodissociation data for many molecules in astrochemical models is based on precomputed, exponentially-attenuated fitted photo rates, which typically assume the opacity of dust

(an important component of such modeling) to be the one characteristic of the average diffuse cloud in the interstellar medium. However, this is unlikely to describe many other astronomical environments, which may lead to significant errors in predicting molecular abundances. To reduce such errors, one may first calculate the cross sections, a fundamental property associated with a given transition of a particular molecule, in order to ultimately compute the photodestruction rates for the particular molecule and environment.

So far cross sections for the photodissociation of HD have been calculated only for the J=0 states, where J is the rotational angular momentum quantum number. Here we have calculated the cross sections corresponding to all rovibrational states of the ground state of HD for the  $B \leftarrow X$  (Lyman) and  $C \leftarrow X$  (Werner) transitions, where X is the ground electronic state of HD and B and C are, respectively, the first two excited electronic states. This required input of potential energy curves for all electronic states, dipole transition moments between them, and once again, rovibrational (binding) energies of the ground state of HD.

## **CHAPTER 2**

## ROVIBRATIONAL ENERGIES OF HD

## 2.1 Theory

In accordance with the principles of quantum mechanics, the internal binding energies of an atom corresponding to the motions of its electrons must take on discrete values. The same applies to a simple diatomic molecule, whose electronic states may be described by potential energy curves such as the ones illustrated in Figure 2.1.

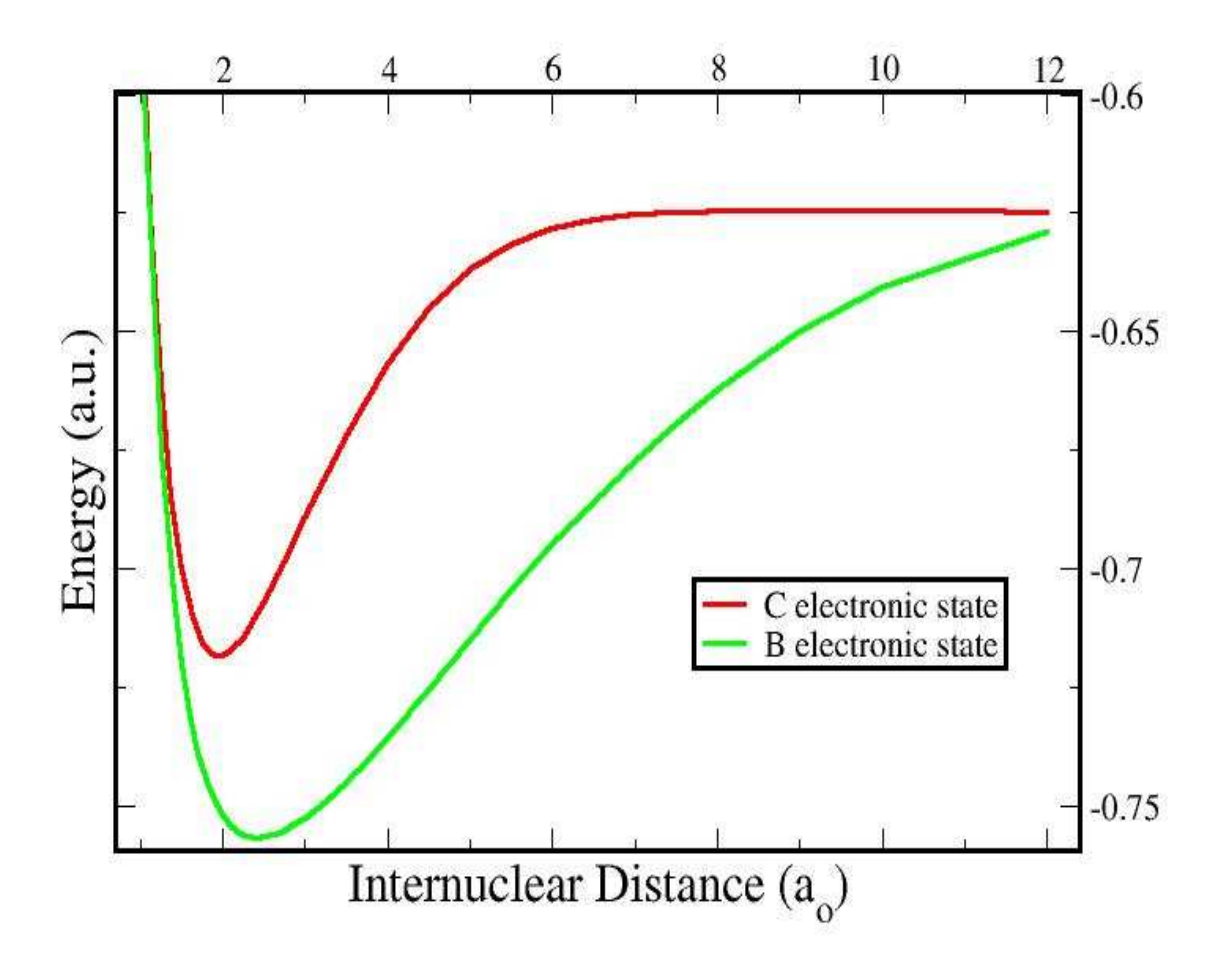


Figure 2.1. Attractive potential energy curves corresponding to the actual B and C electronic states of  $H_2$  as well as HD used in the present work (to scale).

The two curves represent the actual B and C electronic states corresponding to the upper states of the Lyman and Werner transitions, respectively. The same two curves were used for calculation of H<sub>2</sub> (Gay et al., 2008) and HD cross sections, as the mass difference between the two molecules results in negligible corrections to the potential energy functions for the excited states. However, the potential energy curve for the X state of HD, which will be shown in Figure 2.3, differs by an adiabatic correction from the one for H<sub>2</sub>, as the difference in mass affects the nuclear motion and therefore the calculation of rovibrational energies. In this case as well as for the remaining of this thesis - unless otherwise indicated - energy is plotted in units of hartrees (1 hartree = 27.211384566 eV) while internuclear distance is given in units of Bohr radii  $(1 a_0 = 5.291772108 \times 10^{-11} \text{ m})$ . For a stable molecular state, the potential energy shared by the two atoms decreases with decreasing separation, as the nuclei become attracted to the increasingly denser electron cloud, reaches a minimum, and finally, at very small separations, increases exponentially due to the repulsion between the two nuclei. For an unstable or repulsive molecular state (not shown), the energy continues to decrease with increasing nuclear separation never forming a potential well capable of containing bound rovibrational levels.

Aside from the motions of electrons, the nuclei and the molecule as a whole exhibit their own motions. In the harmonic approximation, a diatomic molecule is often represented by two point masses connected by an ideal spring whose equilibrium length corresponds to the minimum potential energy shared by the nuclei. However, unlike an infinite potential well or a perfect harmonic oscillator, the potential well corresponding to an electronic state of a diatomic molecule can hold only a finite number of energy levels. The molecule may rotate as a whole while the nuclei are free to oscillate along their axis. Thus to fully describe the states of a diatomic molecule we must also consider its vibrational and rotational degrees of freedom. Once

again according to the principles of quantum mechanics, the energies due to the vibration and rotation (rovibrational energies) of a diatomic molecule are quantized. They are also contained within a corresponding electronic state. Specifically, each electronic state contains a series of discrete vibrational states which in their own turn contain a series of discrete rotational states, as illustrated in Figure 2.2.

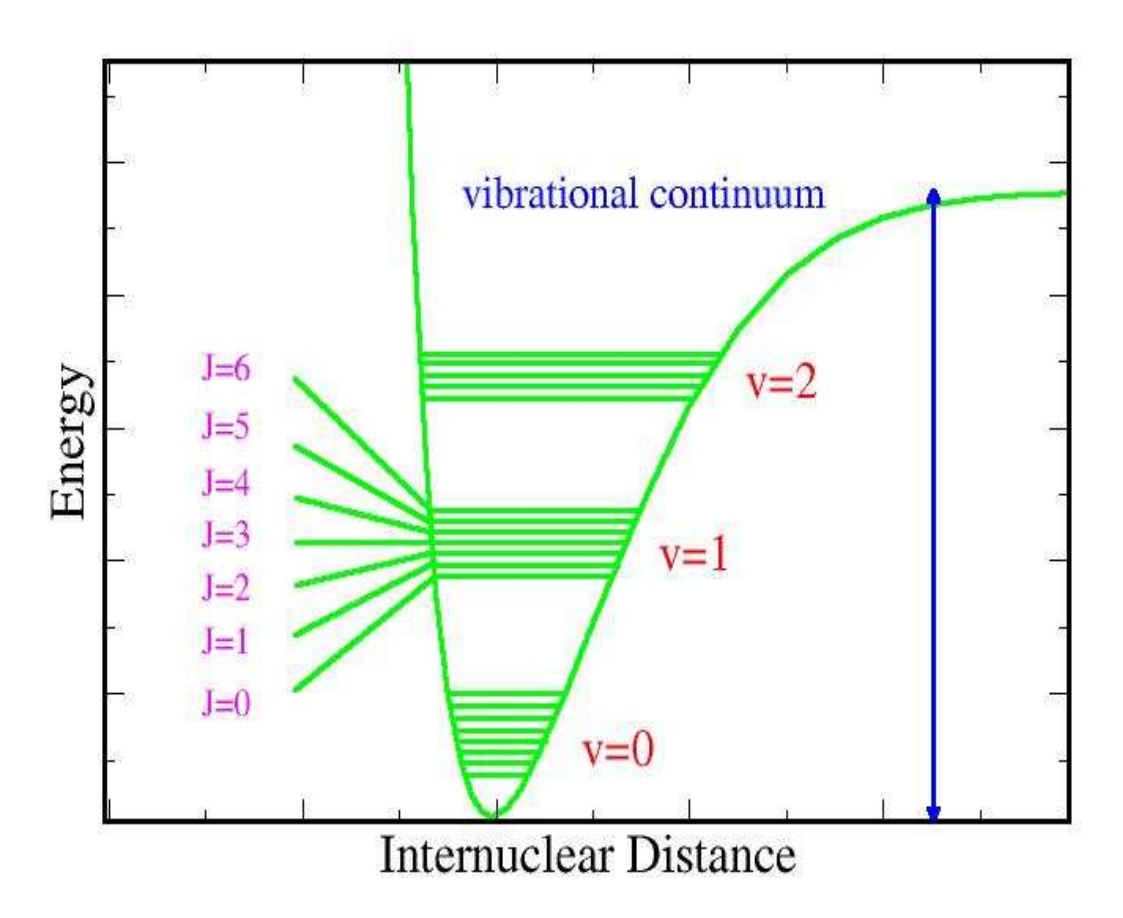


Figure 2.2. Vibrational and rotational energy levels within an electronic state of a diatomic molecule (v and J are, respectively, the vibrational and rotational quantum numbers). The blue vertical line marks the vibrational continuum for this electronic state. The number of rovibrational states as well as the spacing between levels are meant merely to illustrate the concept of vibrational and rotational levels and do not apply to a specific physical system.

This finer structure is revealed by molecular spectra, where lines due to electronic transitions are observed at closer inspection to consist of closely spaced lines due to rotation and vibration. Rovibrational energies are also called binding energies or the energies needed to dissociate the molecule from a particular rovibrational state of a given electronic state. The dissociation energy from an electronic state is equivalent to the binding energy of the v = 0, J = 0 rovibrational state.

For a general diatomic molecule, the Hamiltonian (sum of all kinetic and potential energy terms) may be expressed in space-fixed coordinates as follows:

$$H = -\sum_{K=A,B} \frac{\hbar^2}{2M_K} \nabla^2_K - \frac{\hbar^2}{2m_e} \sum_i \nabla_i^2 + \sum_{i < j} \frac{e^2}{r_{ij}} + \sum_{A < B} \frac{Z_A Z_B e^2}{r_{AB}} - \sum_{i;K=A,B} \frac{Z_K e^2}{r_{iK}}$$
(2.1)

 $M_k$  refers to the masses of the two nuclei, A and B,  $m_e$  is the mass of the electron,  $r_{ij}$  represents the separation between electrons,  $r_{AB}$  the separation between the two nuclei,  $r_{ik}$  is the separation between electrons and nuclei, while  $Z_A$  and  $Z_B$  are the nuclear charges in units of the electron charge, e. The first two terms are, respectively, the kinetic energies of the nuclei and of the electrons. The third and the fourth terms represent the potential energies due to electron repulsion and nuclear repulsion, respectively. Finally, the last term takes into account the potential energy due to the attraction between nuclei and electrons.

Solving the eigenvalue equation,  $\hat{H}\Psi = E\Psi$ , is a difficult task which is somewhat simplified by the Born-Oppenheimer or the so-called adiabatic approximation. In the adiabatic approximation, the total wavefunction  $\Psi$  of the system is written as a product of two wavefunctions, one depending solely on electronic coordinates (and parametrically on internuclear distance) and the other on nuclear coordinates, as in equation 2.2:

$$\Psi(\mathbf{r}, \mathbf{R}) = \psi_{el}(\mathbf{r} \mid R) * \xi_{nuc}(\mathbf{R})$$
(2.2)

Here r refers to the electron coordinates, defined with respect to the center-of-mass of the molecule AB, while R (=  $r_{AB}$ ) is the internuclear vector. The electronic wavefunction  $\psi_{el}(r/R)$  assumes the positions of the nuclei to be fixed, which is a very good approximation, as their motions are much slower than the motions of the electrons. By substituting the above product into the Schrödinger equation, with the Hamiltonian equation (2.1) transformed to center-of-mass coordinates, one arrives at two separate eigenvalue equations, one corresponding to the electronic motion and the other to the nuclear motion. First, the electronic equation is solved for the electronic energy eigenvalues at a number of internuclear distances. This set of eigenvalues forms a potential energy curve which in its turn serves as a potential in the nuclear eigenvalue equation. Each potential energy curve corresponds to a specific electronic state, as the ones illustrated in Figure 2.1.

As the nuclei exhibit both vibration and rotation, the nuclear wavefunction  $\xi_{\text{nuc}}(\mathbf{R})$  is also written as a product of its vibrational and rotational wavefunctions, which correspond, respectively, to the radial and angular parts of the motion.

$$\xi_{nuc}(\mathbf{R}) = \chi_{vJ}(R) / R * \Theta_{JM}(\theta, \varphi)$$
(2.3)

As before, by using separation of variables one arrives at separate equations for  $\Theta_{JM}(\theta,\varphi)$  and  $\chi_{\nu,J}(R)$ , the first of which determines the angular momentum eigenvalues of the system. The second yields the radial nuclear eigenvalue equation (2.4), whose solution determines the vibrational wavefunctions  $\chi_{\nu,J}(R)$  and the rovibrational energies  $E_{\nu,J}$ . Here  $\mu$  is the reduced mass of

the system and is given by  $\frac{M_H M_D}{M_H + M_D}$ , where  $M_H$  is the atomic mass of Hydrogen and  $M_D$  is the atomic mass of the Deuterium atom.  $E_{\rm el}(R)$  is the potential due to the electronic eigenvalues. The equation is in atomic units (in which e=m<sub>e</sub>= $\hbar$ =1, where e is the electric charge of the electron) and is given by

$$\frac{-1}{2\mu} \frac{d^2}{dR^2} \chi_{vJ}(R) + \left[ E_{el}(R) + \frac{1}{2\mu R^2} J(J+1) - E_{vJ} \right] \chi_{vJ}(R) = 0$$
 (2.4)

Due to the centrifugal potential term  $\frac{J(J+1)}{2\mu R^2}$  in equation (2.4), the energy eigenvalues (rovibrational energies)  $E_{\nu J}$  as well as the vibrational wavefunctions  $\chi_{\nu J}(R)$  are functions of both  $\nu$  and J.

#### 2.2 Calculation and results

In order to compute the rovibrational energies of the ground state of HD, the radial nuclear eigenvalue equation (2.4) was solved numerically by a standard Numerov method (Cooley, 1961). A reduced mass of 0.6717112348 amu (Coursey, 2005) (1 amu = 1.66053886 x  $10^{-27}$  kg) was used for HD and the ground state electronic energy eigenvalues  $E_{\rm el}(R)$ , available for an internuclear distance ranging from 0.1 to 100 a<sub>o</sub>, were taken from Wolniewicz (1993, 1995). As mentioned before, Figure 2.3 is a plot of the *X* state potential energy curve for HD as a function of internuclear distance *R*.

Finally, Figure 2.4 shows a plot of the rovibrational energies as functions of vibrational quantum number v while Figure 2.5 plots the energies as functions of rotational quantum number J. There were a total of 400 rovibrational energies found, corresponding to a combination of

vibrational numbers ranging from 0 to 17 (see Figure 2.4) and rotational numbers ranging from 0 to 36 (see Figure 2.5). The dissociation energy of the ground state or equivalently, the binding energy of the v = 0, J = 0 level of the X electronic state, was found to be 0.16588251 hartrees or 4.5138927723 eV. In units of cm<sup>-1</sup>, this value works out to be 0.36406998 x  $10^5$ . This is in very good agreement with the experimental value of 0.3640583 x  $10^5$  cm<sup>-1</sup> obtained by Balakrishnan et al. (1993) by analysis of HD fluorescence excitation spectra. Our calculation also agrees with the previous theoretical result of 0.36405784 x  $10^5$  cm<sup>-1</sup> obtained by Kolos et al. (1986).

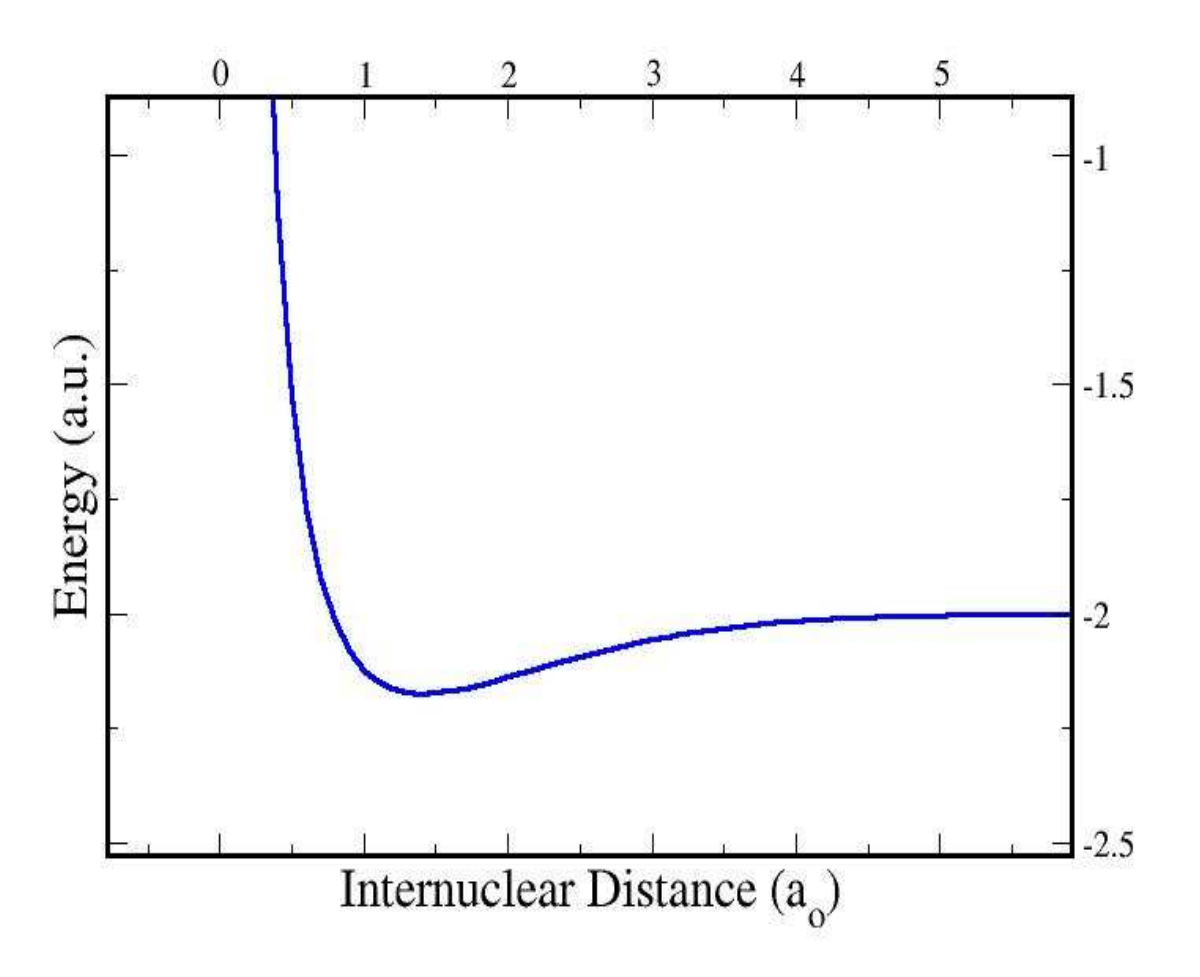


Figure 2.3. Potential energy curve corresponding to the *X* electronic state of HD as a function of internuclear distance.

Due to its lower reduced mass (0.503912516 amu), the binding energy for the ground state of  $H_2$  is slightly less deep - 0.164566118 hartrees or 4.4780719234 eV (Perry, 2005) - than the one for HD. Thus as expected, the number of rovibrational levels contained in the ground state of HD exceeded the one for  $H_2$  (400 versus 301). The complete list of HD binding energies in units of hartrees as well as in cm<sup>-1</sup> by their corresponding v and J is provided in the Appendix. The number of rotational levels decreases with increasing v, 37 being the highest (v = 0) and 2 being the lowest (v = 17).

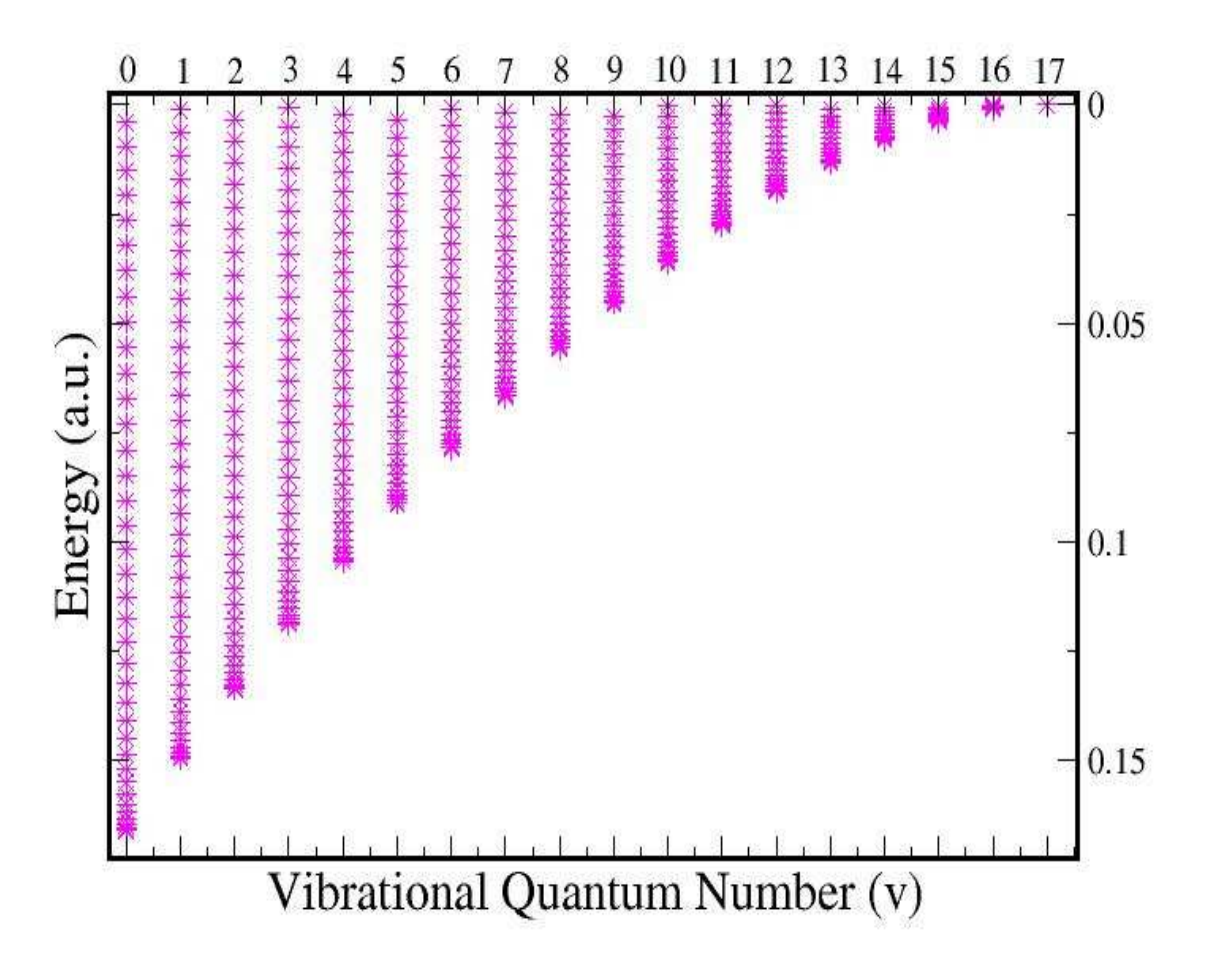


Figure 2.4. Rovibrational binding energies of the ground (X) state of HD versus corresponding vibrational quantum number  $\nu$ .

Each vertical set of data points in Figure 2.4 corresponds to a particular vibrational level of the ground state and contains all its rotational levels with J increasing upward. Thus the lowest point in the lower left-hand corner corresponds to the v = 0, J = 0 state while the highest point in the upper right-hand corner corresponds to the v = 17, J = 1 state.

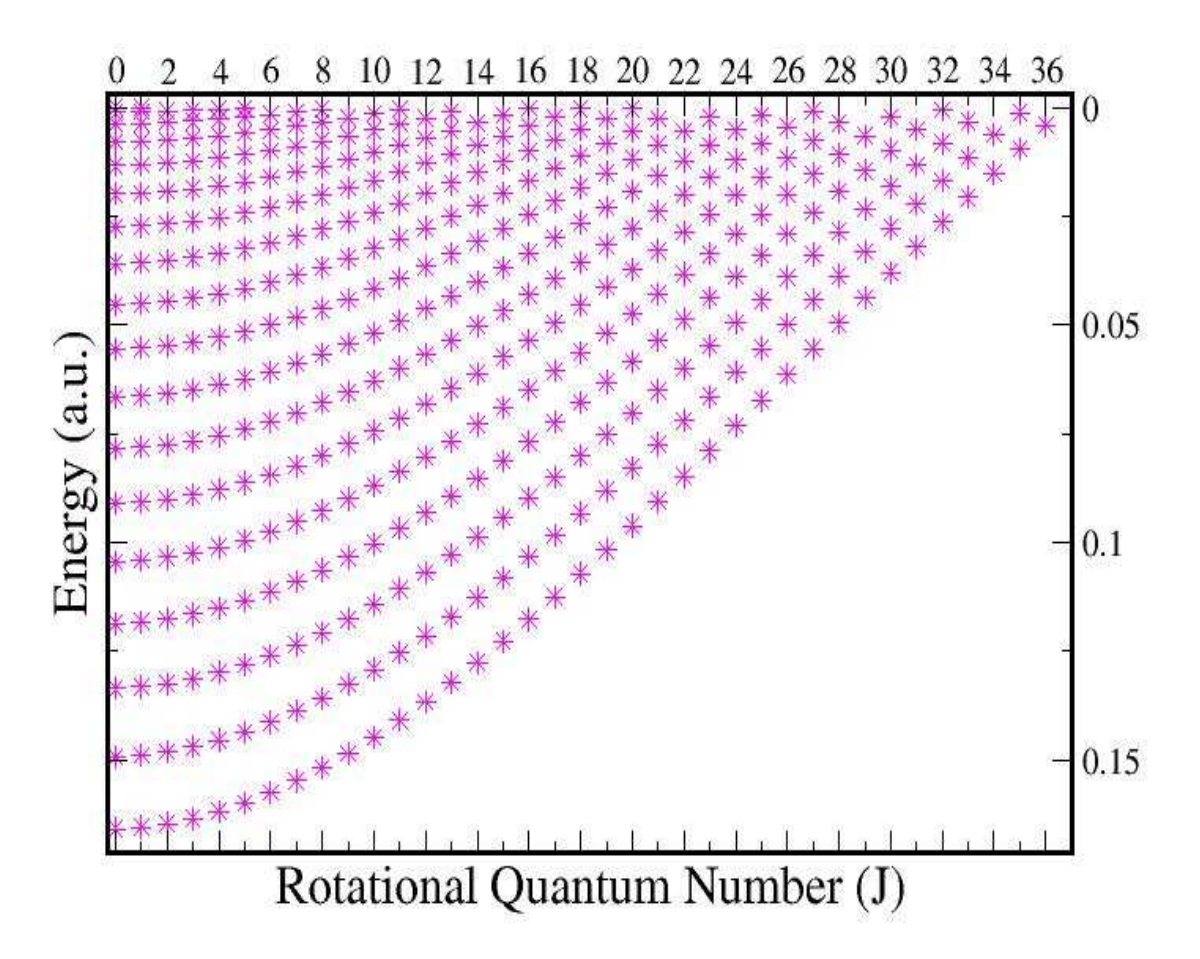


Figure 2.5. Rovibrational binding energies of the ground (X) state of HD versus corresponding rotational quantum number J.

In Figure 2.5 v increases upward and J increases toward the right, thus the lowest point in the lower left-hand corner corresponds to the v = 0, J = 0 state while the highest point in the upper

right-hand corner corresponds to the v = 0, J = 36 state. As progressively higher rovibrational states are increasingly less bound, an implicit negative sign should be assumed for all of the energy values. However, as equation (3.2) will illustrate, the cross sections are functions of the difference between energy levels and thus the sign may be safely ignored in their calculations. Once rovibrational energies were obtained, they were adopted for photodissociation calculations for the Lyman and Werner transitions of HD.

#### **CHAPTER 3**

#### PHOTODISSOCIATION OF HD

#### 3.1 Theory

Molecular photodissociation is the process through which the chemical bond between two or more atoms is broken as a result of the interaction with one or multiple photons.

The photons excite the molecule from the ground or a lower state into an upper electronic state, which if repulsive, invariably leads to dissociation. Photodissociation may also take place from the continuum of a bound upper electronic state. This is the mechanism by which photodissociation through the Lyman and Werner transitions occurs. A necessary condition for photodissociation to occur is the photon energy exceeding the energy needed for the molecule to transition from a ground-state rovibrational level into the upper-most rovibrational level of the upper electronic state. Otherwise, the molecule simply transitions into a bound level of the upper state without dissociating. The excess photon energy, i.e. the difference between the total energy of the photon and the energy needed to reach the continuum of the upper state, is then converted into translational and internal (e.g., electronic) energies of the separate atoms (Schinke, 1993).

The photodissociation of diatomic molecules can occur through several mechanisms, as discussed by van Dishoeck (1988). With direct photodissociation, the system, initially in a bound state of an attractive potential, absorbs a photon which sends it into a repulsive upper state or into the continuum of a bound upper state. As spontaneous emission back to the original state is comparatively slow, this invariably leads to the dissociation of the molecule (van Dishoeck, 1988). In the case of pre-dissociation, a bound level of an excited state is an intermediate step between the initial state and the final repulsive state of a different symmetry, which crosses and is coupled with the intermediate state. Yet another mechanism is the so-called coupled states

photodissociation, in which the continuum of a repulsive state of the same symmetry affects but does not cross the intermediate excited state. Finally, in the case of spontaneous radiative dissociation, a photon is emitted as the system makes a transition from a vibrational level of an upper state into the vibrational continuum of the ground state, an intermediate state, or a lower repulsive state. This is the primary dissociation process for HD as well as for  $H_2$  when the photon energy ranges between approximately 11 and 13.6 eV for the v=0, J=0 level. In the case of direct photodissociation, the cross section is continuous as a function of wavelength and its shape reflects the lower state wavefunction, while for pre-dissociation, coupled-states photodissociation, and spontaneous radiative dissociation it consists of a series of broadened peaks, a continuous background with superimposed peaks, and a series of narrow peaks, respectively. The Lyman ( $B \leftarrow X$ ) and Werner ( $C \leftarrow X$ ) transitions of HD, i.e. the two transitions considered in this paper, are both examples of direct photodissociation. The remaining of this chapter deals with a more quantitative way of looking at cross sections and applies strictly to direct photodissociation.

In order to compute photodissociation rates for a particular environment, one first calculates the cross sections associated with a particular transition of the given molecule. For our purposes, the concept of a cross section is used to describe the likelihood of a molecule dissociating via a transition from a particular rovibrational state corresponding to the lower electronic state into the continuum of the upper electronic state. In order to obtain cross sections, it is necessary to first compute the wavefunctions corresponding to the two electronic states, namely the vibrational and the continuum wavefunctions. As covered in Chapter 2, equation (2.4) may be solved to obtain the vibrational wavefunctions  $\chi_{\nu,l}(R)$ . As this applies strictly to bound states of an attractive potential, in considering repulsive potentials or regions above the

dissociation limit of an attractive potential curve (Kirby & van Dishoeck, 1988), equation 3.1 must instead be solved for the continuum wavefunctions  $\chi_{k,l}(R)$ .

$$\frac{-1}{2\mu} \frac{d^2}{dR^2} \chi_{kJ}(R) + \left[ E_{el}(R) + \frac{1}{2\mu R^2} J(J+1) + E_k \right] \chi_{kJ}(R) = 0$$
(3.1)

 $E_k$  is the relative kinetic energy of the two dissociating atoms and is given by  $k^2/2\mu$ , where k is the wave number relating to the momentum of the two atoms.

Finally, the cross sections as functions of photon energy are given by

$$\sigma(\Delta E_{k'J'v''J''}) = \frac{2}{3} \frac{\pi e^2}{mc} g\Delta E_{k'J'v''J''} \left| \left\langle \chi_{k'J'}(R) \middle| D_{fi}(R) \middle| \chi_{v''J''}(R) \right\rangle \right|^2$$
(3.2)

The primed superscripts refer to the final state of the molecule while the double primed superscripts refer to its initial one.  $\Delta E_{k'J'v''J''}$  is the photon energy,  $\chi_{k'J'}(R)$  represents the continuum wavefunction, i.e. the solution to equation (3.1), and  $\chi_{v''J''}(R)$  is the initial state wavefunction, i.e. the solution to equation (2.4).  $D_{fi}(R)$  is the electric dipole transition moment, which governs the strength or probability of a transition between the two electronic states due to photon absorption. It is given by equation (3.3):

$$D_{fi}(R) = \int \psi^*_f(\mathbf{r} \mid R) \sum e_j r_j \psi_i(\mathbf{r} \mid R) d\mathbf{r}$$
(3.3)

As before,  $\mathbf{r}$  and R refer, respectively, to electron and nuclear coordinates, while  $\psi_f^*(\mathbf{r}/R)$  and  $\psi_i(\mathbf{r}/R)$  are the complex conjugate of the final state electronic wavefunction and the initial state electronic wavefunction, respectively. Moreover,  $\frac{2}{3} \frac{\pi e^2}{mc}$  is a constant equal to the numerical

value of  $2.69 \times 10^{-18}$ , assuming that the photon energy, wavefunctions, and dipole transition moment are in atomic units. g represents a degeneracy factor given by

$$g = \frac{2 - \delta_{0,\Lambda' + \Lambda''}}{2 - \delta_{0,\Lambda''}} , \qquad (3.4)$$

where  $\Lambda$  is the quantum number corresponding to the projection of the total electronic orbital angular momentum along the internuclear axis (Kirby and van Dishoeck, 1988) and is numerically equal to 1 for the C electronic state and 0 for the X and B electronic states. Therefore A is equal to 1 for the A transition and 2 for the A transition.

Once the cross sections for a particular transition are computed, the direct photodissociation rates may be obtained by integrating the product of the cross sections and the mean intensity of the radiation field of interest. The product is integrated over the range of photon wavelength for which the cross sections and mean intensity are non-zero (Kirby & van Dishoeck, 1988). Equation (3.5) gives the photodissociation rate  $\kappa_{\nu}^{pd}$  corresponding to an environment of mean intensity  $I(\lambda)$  and cross sections  $\sigma_{\nu}$  in units of s<sup>-1</sup>:

$$\kappa_{\nu''}^{pd} = \int \sigma_{\nu''}(\lambda) I(\lambda) d\lambda \tag{3.5}$$

### 3.2 Calculations and results

In the case of photodissociation through the Lyman and Werner transitions, the process may occur through either of the two following channels:

Channel 1:  $HD + photon \rightarrow H(1s^1) + D(2p^1)$ 

Channel 2:  $HD + photon \rightarrow H(2p^1) + D(1s^1)$ 

In the X state, the electronic configuration of both Hydrogen and Deuterium corresponds to the  $1s^1$  subshell, where the first number denotes the principal quantum number n or energy level, the second is the azimuthal quantum number indicating orbital angular momentum l ( $s \leftrightarrow l = 0$ ,  $p \leftrightarrow l = 1$ ), and the superscript refers to the number of electrons in the subshell. Following the photodissociation of the molecule through absorption into the continua of the B and C states, Hydrogen and Deuterium may be found, respectively, in the  $1s^1$  and  $2p^1$  subshells or in the  $2p^1$  and  $1s^1$  subshells, as shown above. Our method does not distinguish between the two channels, as it is aimed solely at determining the likelihood of photodissociation occurring through the Lyman and Werner transitions, without regard to the subsequent states of the individual atoms.

As with the calculation of the rovibrational energies, we numerically solved equations (2.4), (3.1), and (3.2) for the vibrational wavefunctions, continuum wavefunctions, and cross sections, respectively, by a Numerov method using a legacy code written in Fortran. As the calculations involved merely the two uncoupled channels above, they were highly efficient from a computational standpoint. The entire set of calculations for cross sections corresponding to either the B or the C electronic state and from all rovibrational levels of the ground state of HD was performed on a typical Athlon compute node in approximately 12 hours. Electric dipole transition moments (shown in Figures 3.1 and 3.2) were available for an internuclear distance ranging from 1 to 12  $a_0$  (Dressler & Wolniewicz, 1985). They are somewhat different from each other, as the X, B, and C electronic states correspond, respectively, to  $\Sigma$ ,  $\Sigma$ , and  $\Pi$  types of covalent bonding.  $\Sigma$  bonding occurs when the electronic orbitals overlap along the plane

containing the atoms, while the weaker  $\Pi$  bond corresponds to a lateral overlapping of the orbitals. The transition moments alone cannot be used to predict the shape and size of the Lyman and Werner cross sections, but they do play a role in determining their relative magnitudes.

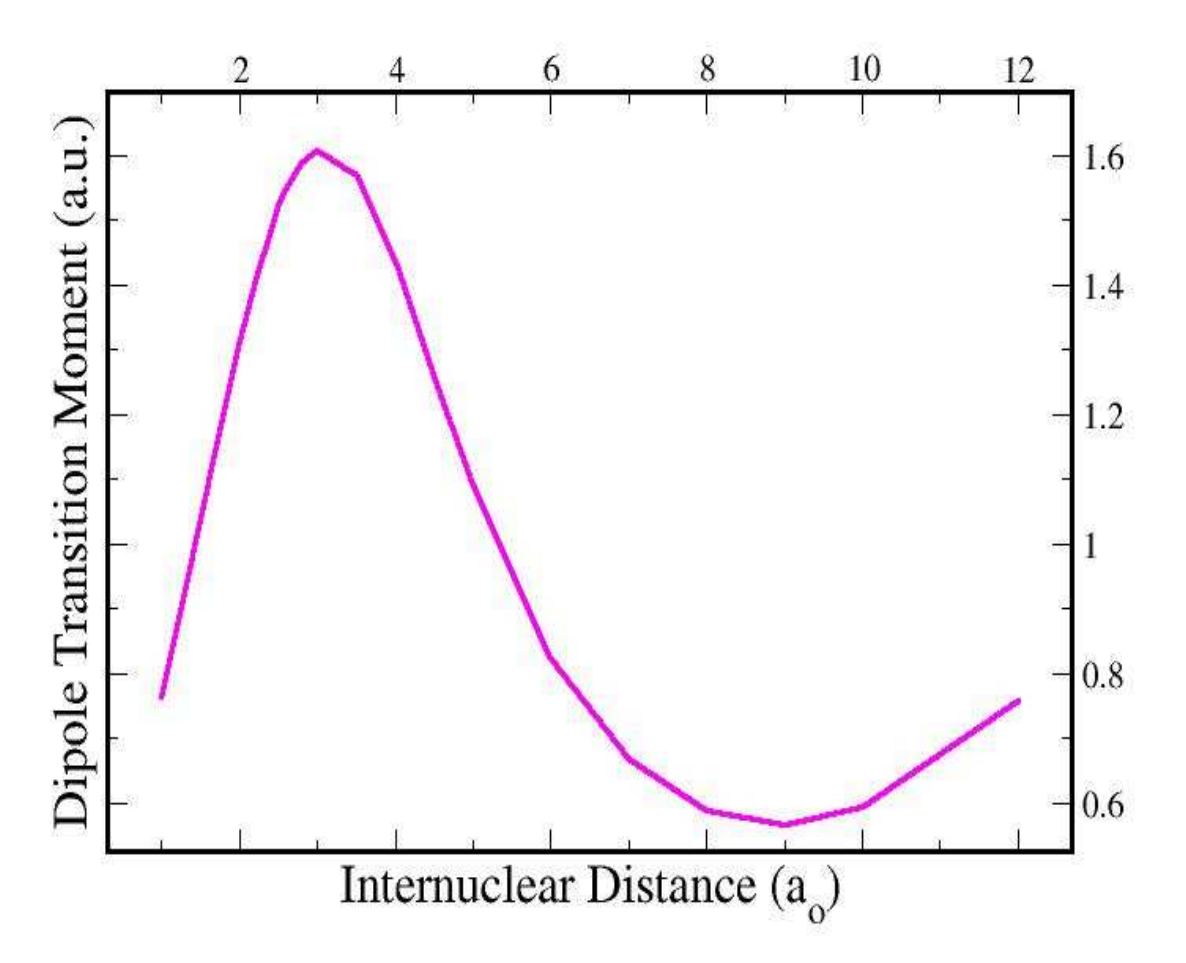


Figure 3.1. Electric dipole transition moment as a function of internuclear distance for the Lyman transition of HD.

Further input consisted of potential energy curves, which were available for the B state (Kolos & Wolniewicz, 1968) and C state (Kolos & Wolniewicz, 1965) for an internuclear distance ranging from 1 to 12  $a_0$ . As before, the X state potential energy data was available for a range of 0.1 to

100 a<sub>o</sub> (Wolniewicz, 1993, 1995). The potential curves for all three states were shown in Figures 2.3 (*X*) and 2.1 (*B* and *C*).

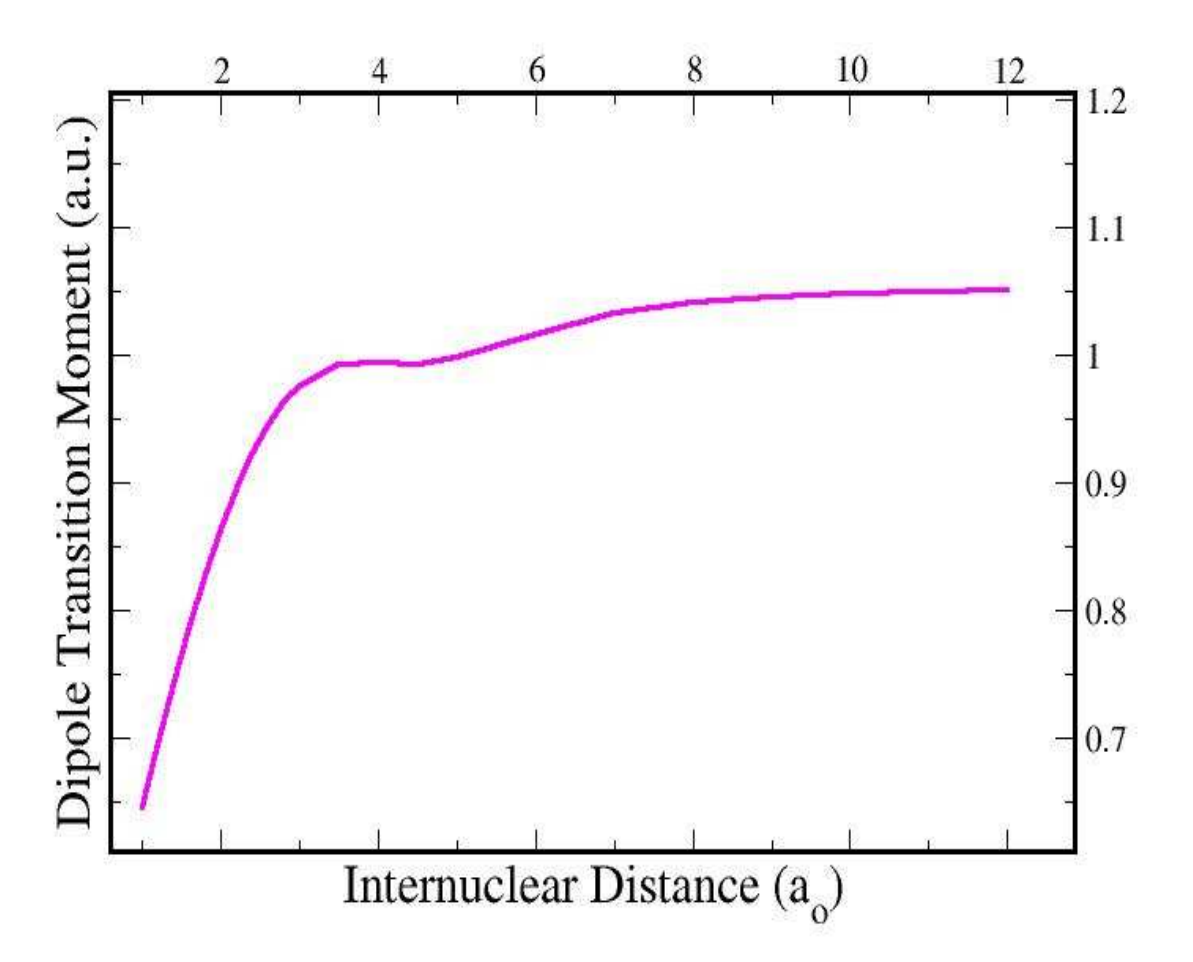


Figure 3.2. Electric dipole transition moment as a function of internuclear distance for the Werner transition of HD

Given all necessary potential energy and transition moment data as well as the ground state rovibrational energies, we computed the photodissociation cross sections as functions of photon wavelength ranging (in this case) from 100 Å to the dissociating threshold from each rovibrational state. However, we illustrate first in Figure 3.3 the typical behavior of the radial

wavefunctions. Studying the wavefunctions provides insight into the behavior of the cross sections, particularly their oscillating pattern at higher v and J.

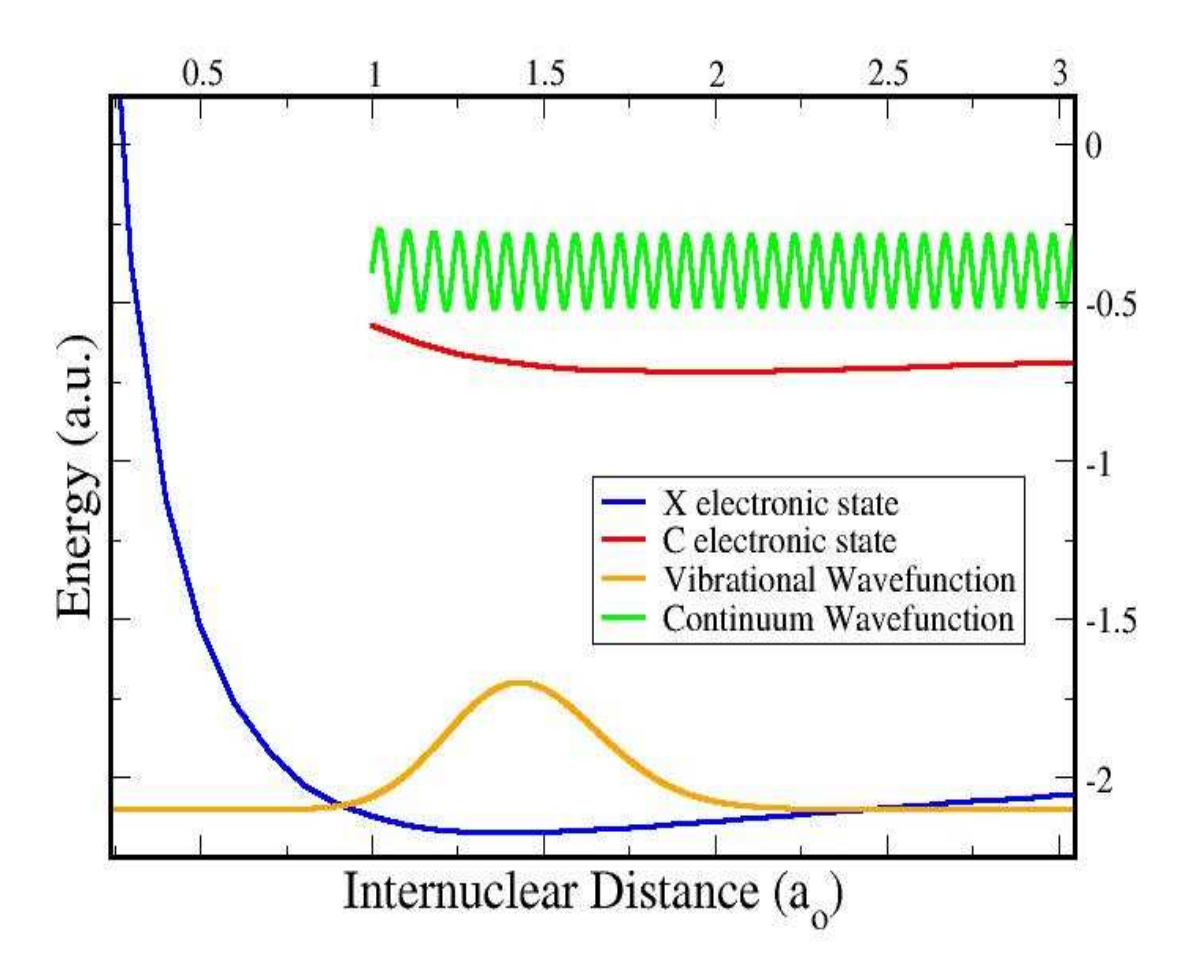


Figure 3.3. X and C potential energy curves with corresponding vibrational and continuum wavefunctions superimposed.

Figure 3.3 is a plot of the ground state vibrational wavefunction,  $\chi_{o,o}$ , and the upper state (C in this case) and continuum wavefunction,  $\chi_{kJ}$ . For v greater than zero, vibrational wavefunctions exhibit nodes which increase in number with increasing v. More specifically, the number of nodes in the probability density distribution given by  $|\chi_{vJ}(R)|^2$  precisely equals the vibrational

quantum number v. On the other hand, continuum wavefunctions behave sinusoidally. Equation (3.5) gives their asymptotic behavior for large separations:

$$\chi_{kJ}(R) \sim \left(\frac{2\mu}{\pi k}\right)^{1/2} \sin(kR + \eta), \qquad (3.5)$$

where  $\eta$  is the elastic scattering phase shift (Kirby & van Dishoeck, 1988).

The following Figures show some of the partial cross sections obtained for various combinations of v and J. Figure 3.4 is a plot of partial cross sections corresponding to v = 0 and several rotational quantum numbers J for the Lyman ( $B \leftarrow X$ ) transition of HD. Figure 3.5 shows the cross sections from the same rovibrational levels of the ground state for the Werner ( $C \leftarrow X$ ) transition of HD. In this, as in all remaining Figures, the cross section is plotted as a function of photon wavelength, while the abscissa is in units of Angstroms ( $1 \text{ Å} = 10 \text{ x } 10^{-10} \text{ m}$ ) and the ordinate in units equivalent to Angstroms squared. The cross sections were calculated from a photon wavelength of 100 Å up to the dissociation threshold, i.e. the wavelength (or equivalently, the energy) at which photodissociation through these particular channels satisfies conservation of energy. In Figures 3.4 and 3.5, the cross sections are largest around the threshold and decrease steadily with decreasing wavelength.

The energy of a photon is given by  $\frac{hc}{\lambda}$ , where h is Planck's constant, c is the speed of light, and  $\lambda$  the photon wavelength. The fact that the cross sections decrease to virtually zero at higher energies does not imply that a more energetic photon is less likely to dissociate the molecule. Rather, at higher energies, a transition into a rovibrational level or continuum of a higher electronic state (from where it might dissociate) may be more probable.

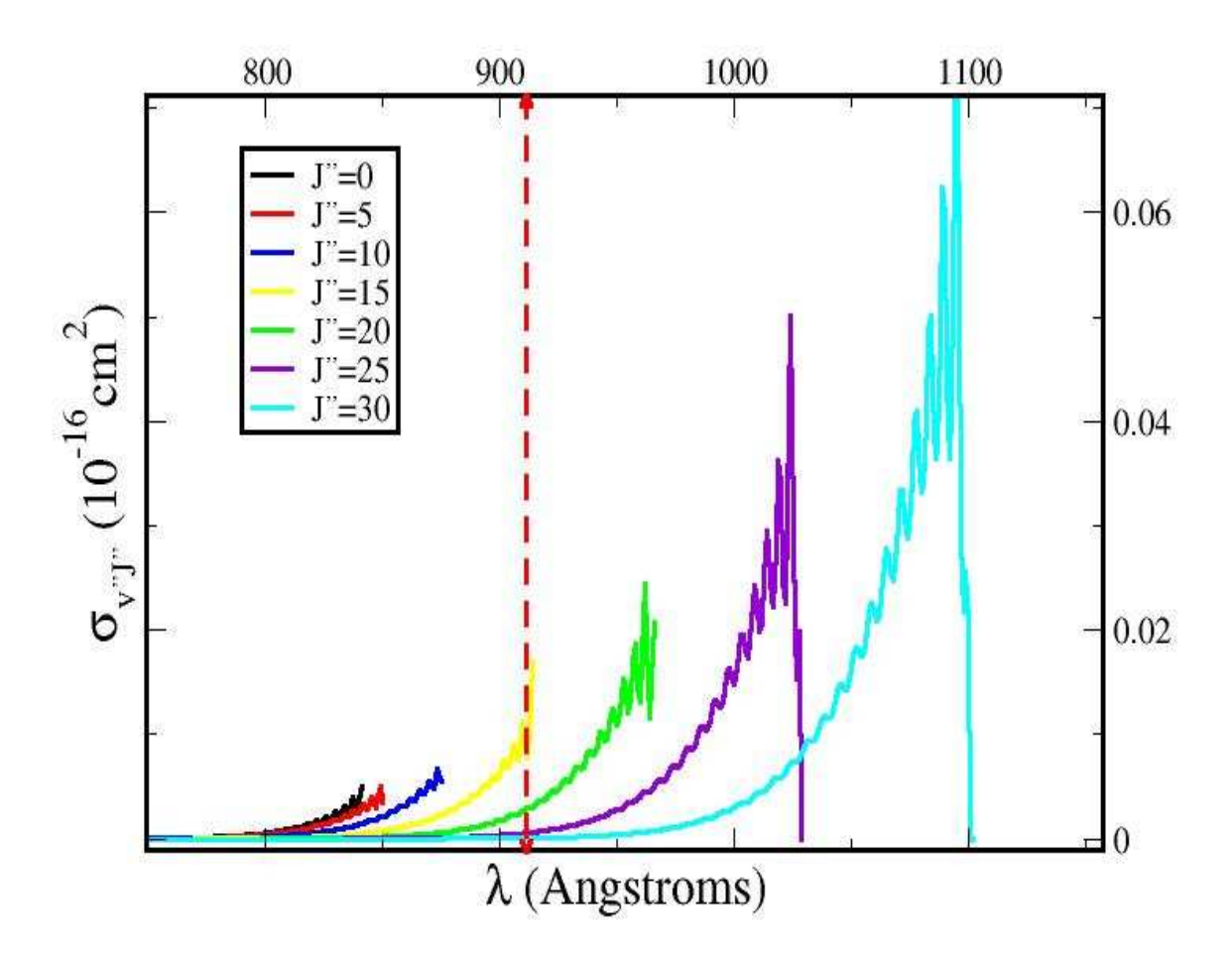


Figure 3.4. Partial cross sections for the Lyman transition of HD from several rotational levels corresponding to vibrational quantum number v=0 of the ground electronic state. In this, as in all subsequent Figures, the red dashed line ( $\lambda=911.3~\text{Å}$ ) marks the Lyman edge for atomic Hydrogen.

However, in the present work we are not considering photodissociation of HD through all possible channels. The computed cross sections apply strictly to photodissociation through the  $B \leftarrow X$  and the  $C \leftarrow X$  transitions, i.e. transitions from a bound rovibrational level of the ground electronic state into the continuum of the B or C electronic state.

In the interstellar medium (ISM), the average radiation field is severely depleted for wavelengths shorter than 911.3 Å (the Hydrogen Lyman edge) due to continuum absorption by atomic Hydrogen (Draine, 1978). Therefore, the photo-destruction of HD via direct photodissociation from the v = 0, J = 0 rovibrational level of its ground state pays no role in this particular environment. However, as Figure 3.4 illustrates, photodissociation becomes significant for v = 0 and J greater than 15. Later Figures will also illustrate that HD photodissociation cross sections are non-zero for ISM radiation for J = 0 and v greater than 3 as well as for other

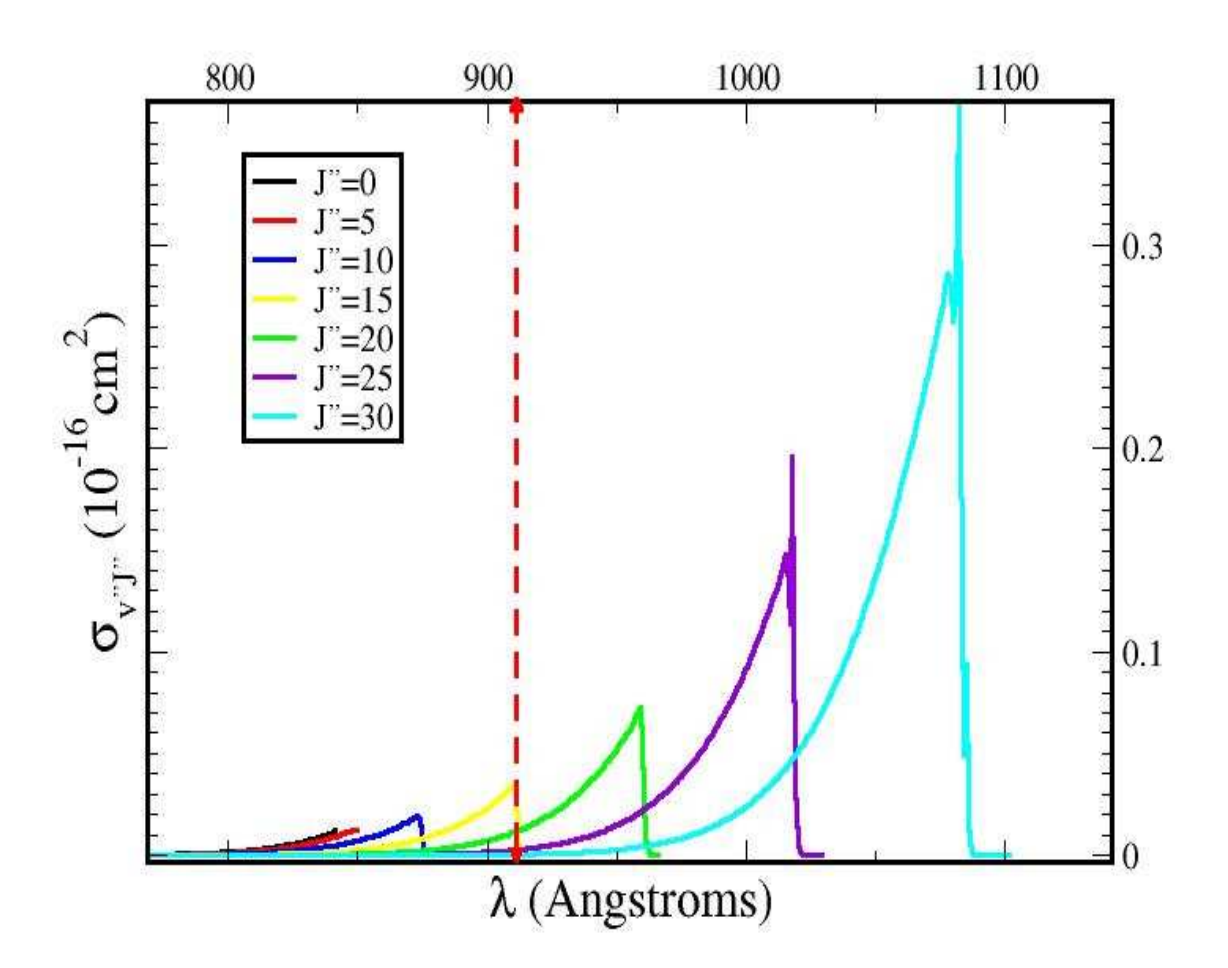


Figure 3.5. Partial cross sections for the Werner transition of HD from several rotational levels corresponding to vibrational quantum number v = 0 of the ground electronic state.

combinations of excited v and J. On the other hand, we note that the short wavelength radiation is intense in a variety of astronomical environments, including protoplanetary disks, and therefore direct photodissociation from all v and J could be a dominant destruction mechanism for HD.

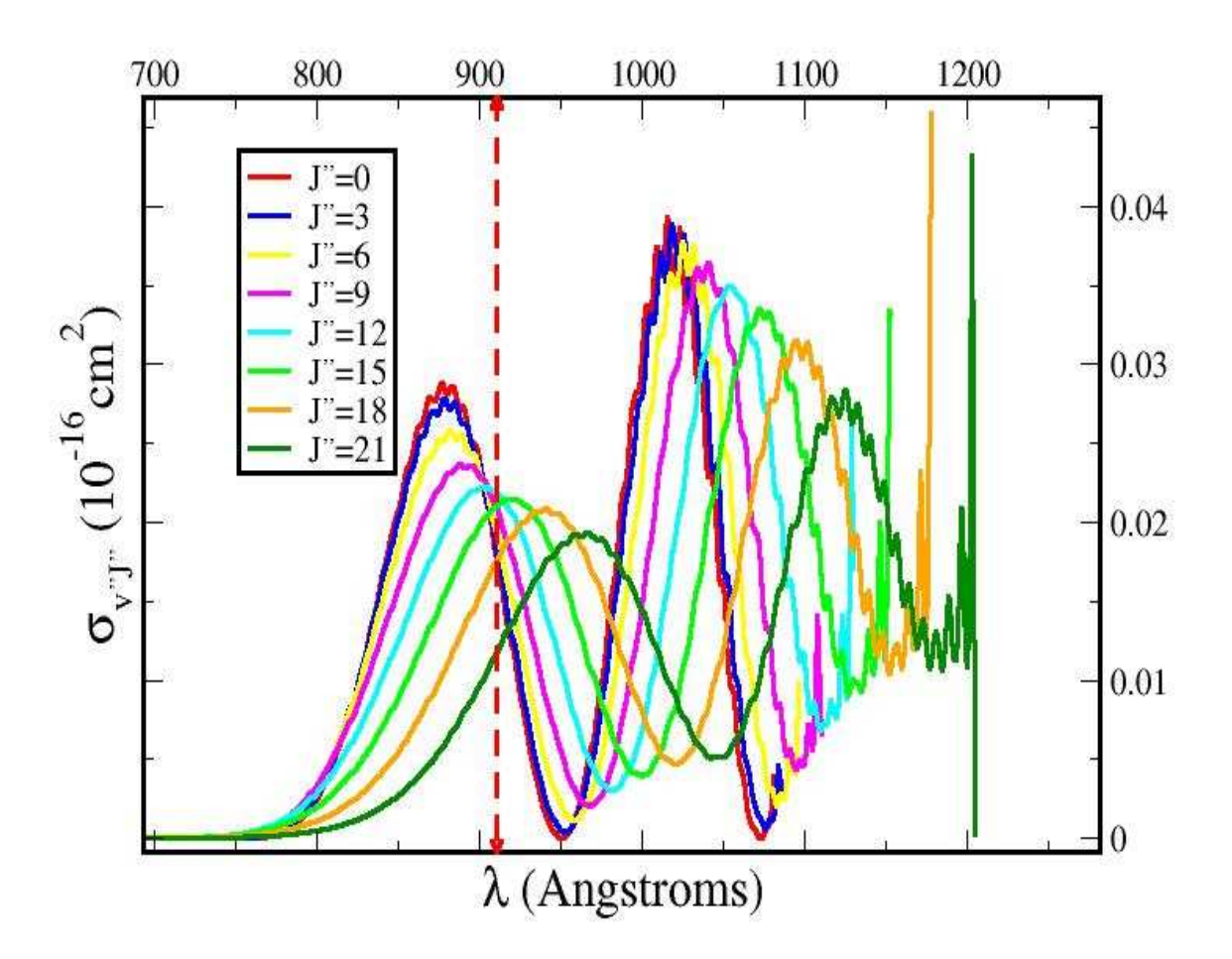


Figure 3.6. Partial cross sections for the Lyman transition of HD from several rotational levels corresponding to vibrational quantum number v = 9 of the ground electronic state.

Figures 3.6 and 3.7 give the partial cross sections for the Lyman and Werner transitions of HD from the rovibrational levels of the X state corresponding to v = 9 and several J. Here the cross sections do not decrease uniformly with decreasing wavelength but rather, they exhibit

several oscillations which tend to damp down toward higher energies. As mentioned before, this is due to the sinusoidal behavior of the continuum wavefunction and, perhaps more importantly, to the behavior of the vibrational wavefunction, which exhibits more nodes and antinodes as *v* increases.

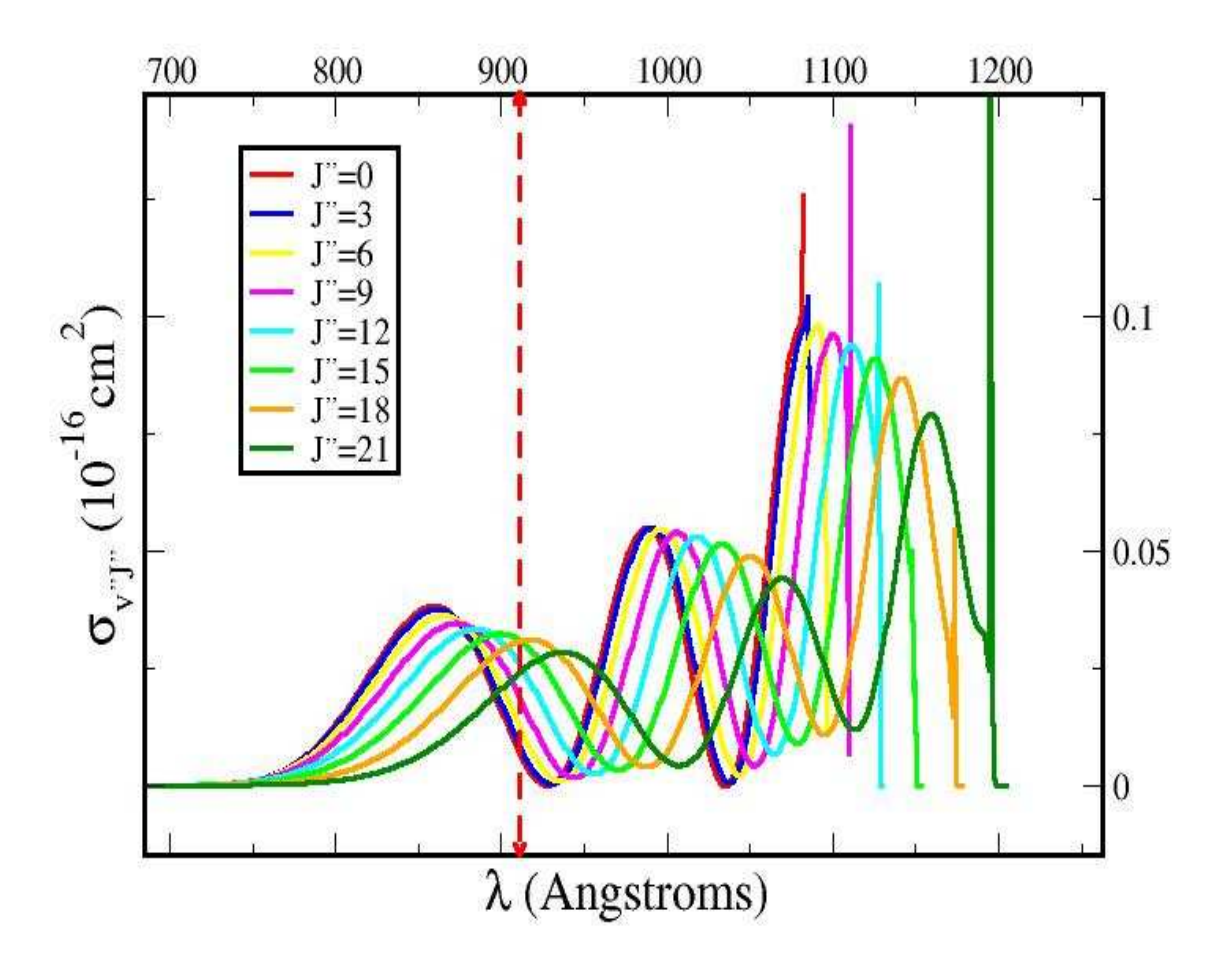


Figure 3.7. Partial cross sections for the Werner transition of HD from several rotational levels corresponding to vibrational quantum number v = 9 of the ground electronic state.

The superimposed sharp peaks in some of the cross sections are known as orbiting resonances.

They occur when the energy of the outgoing particles (the Hydrogen and Deuterium atoms)

aligns with the energy of a quasi-bound *B* or *C* state. Classically, one can envision the two atoms

orbiting each other for a number of periods in the B or the C electronic state (hence the name "orbiting resonances"), as the system is nearly trapped by a barrier due to the centrifugal potential energy term in equation (3.1). For internuclear distances smaller than the barrier, the amplitude of the continuum wavefunction becomes very large, which in turn enhances the cross section.

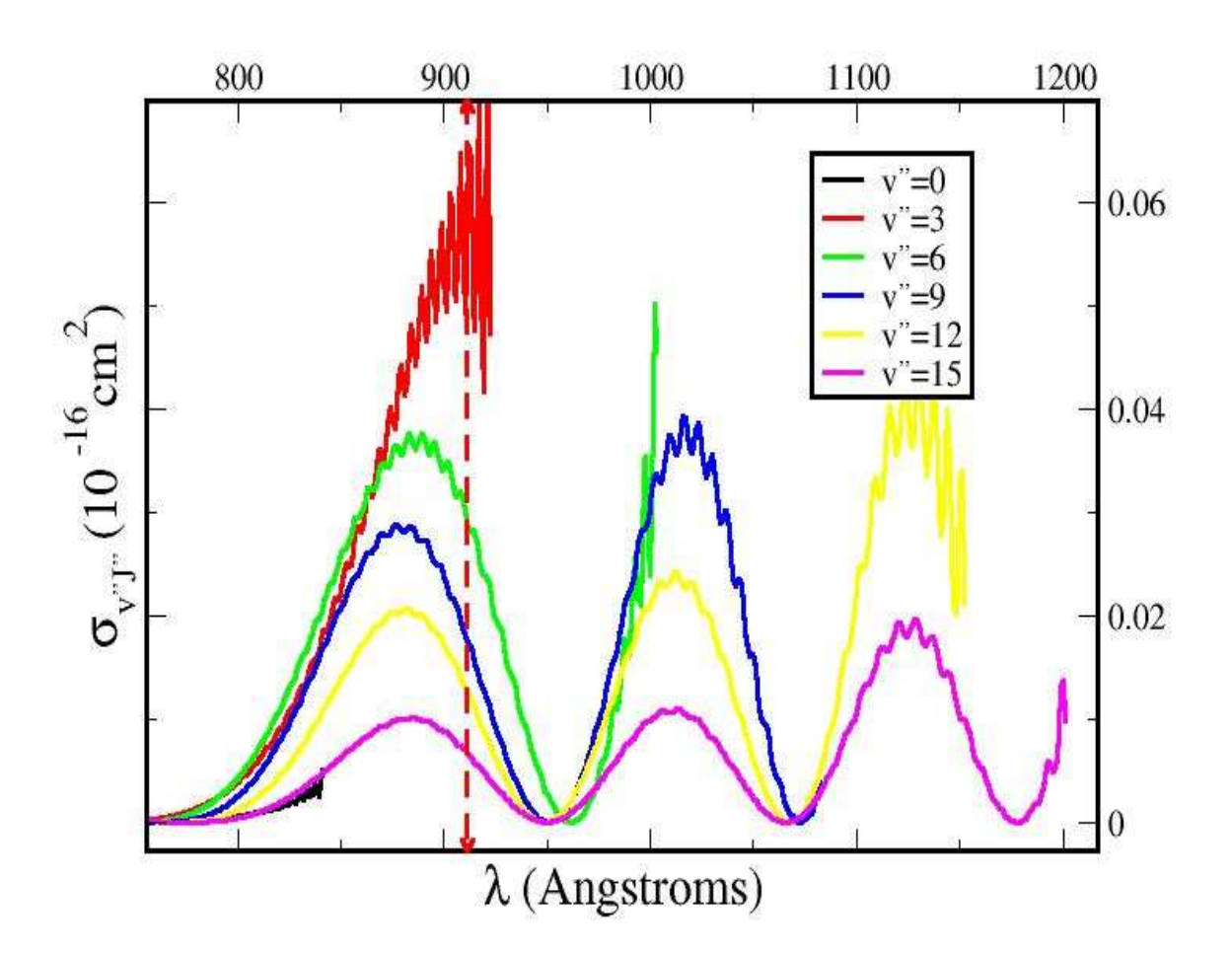


Figure 3.8. Partial cross sections for the Lyman transition of HD from several vibrational levels corresponding to rotational quantum number J = 0 of the ground electronic state.

Figures 3.8 and 3.9 present some of the cross sections for the Lyman and Werner transitions of HD corresponding to J = 0 and several vibrational levels of the ground electronic

state. As in the previous four Figures, where thresholds shifted to higher wavelengths with increasing J, here thresholds again shift to the right with increasing v. This is because a lower amount of energy is required to reach the continuum of the upper state from a higher rovibrational level of the ground state.

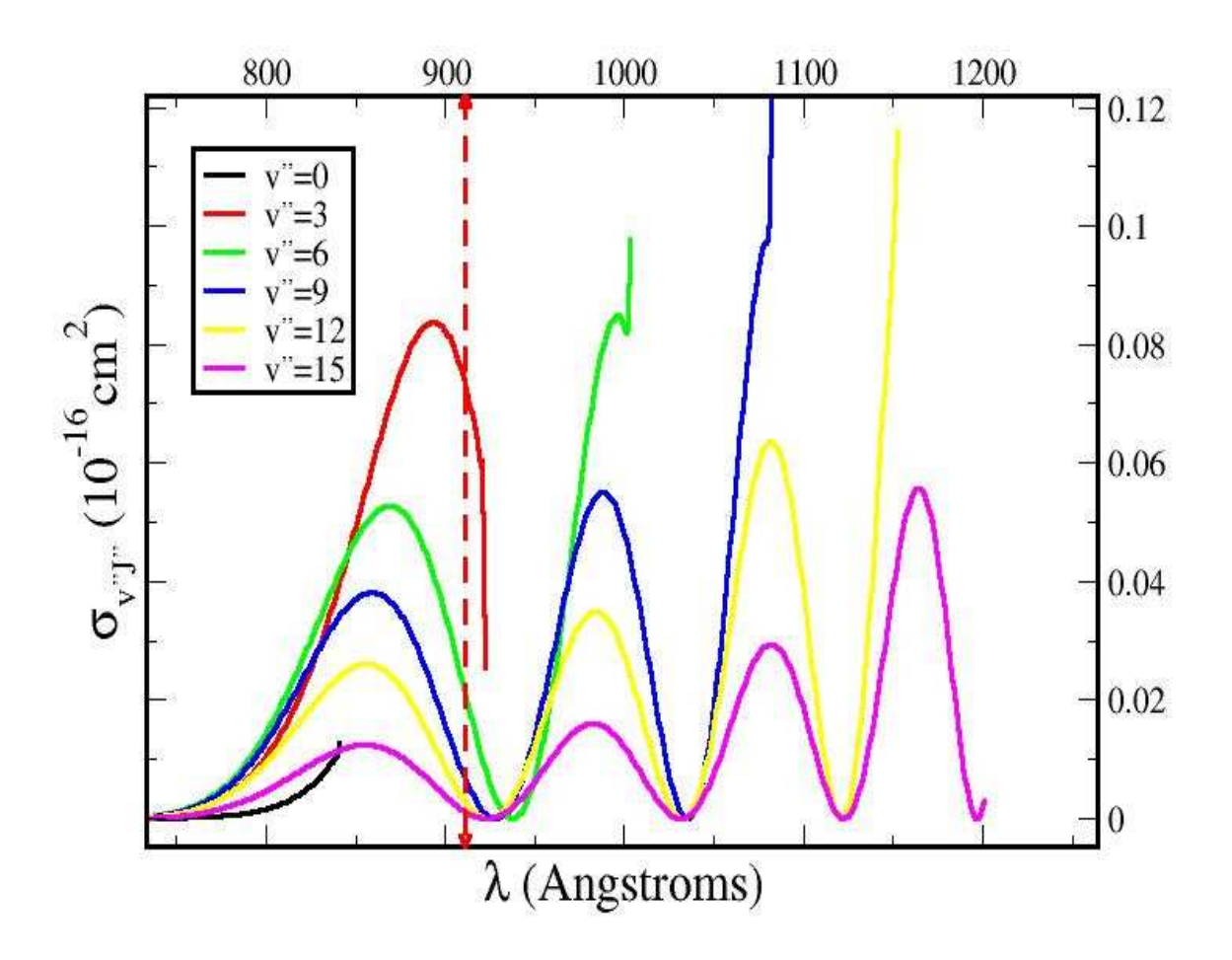


Figure 3.9. Partial cross sections for the Werner transition of HD from several vibrational levels corresponding to rotational quantum number J = 0 of the ground electronic state.

Figures 3.10 (Lyman transition) and 3.11 (Werner transition) show some of the cross sections corresponding to J = 9 and several vibrational levels of the ground state. As expected, the difference in shift between J = 0 and J = 9 cross sections for the same v is much smaller than

the difference in shift between v = 0 and v = 9 cross sections for the same J. This is because the spacing between rotational levels within a given v level is much tighter compared to the spacing between different vibrational levels (for any given J).

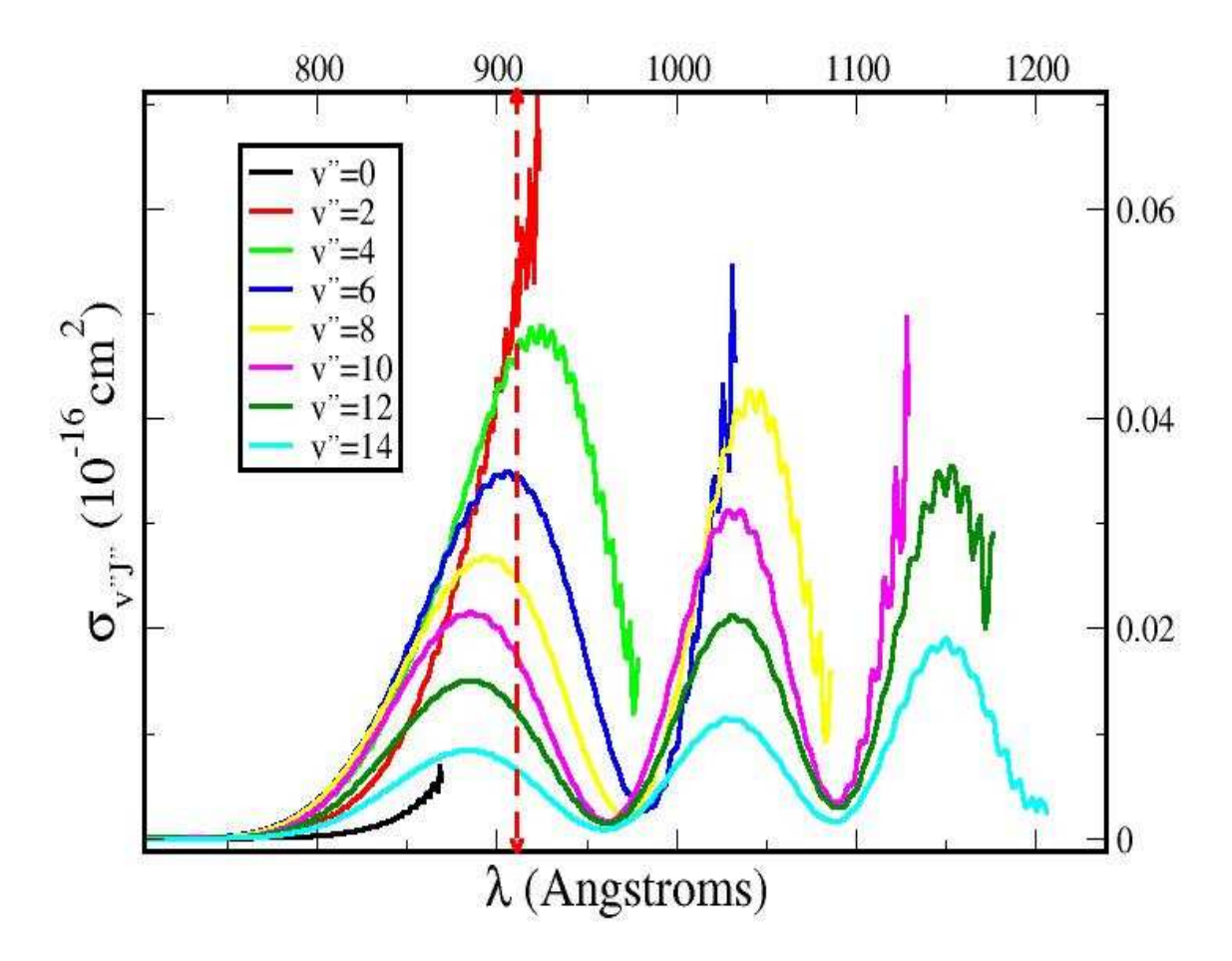


Figure 3.10. Partial cross sections for the Lyman transition of HD from several vibrational levels corresponding to rotational quantum number J = 9 of the ground electronic state.

As is evident from all Figures, cross sections are zero for wavelengths larger than the threshold. Beyond this point, there is not sufficient energy for the molecule to transition from a rovibrational level of the ground state into the continuum of the upper state. The photon might possess enough energy to bump the molecule up to a higher rovibrational level of the same

electronic state, but that would nevertheless constitute a bound state and photodissociation would not occur.

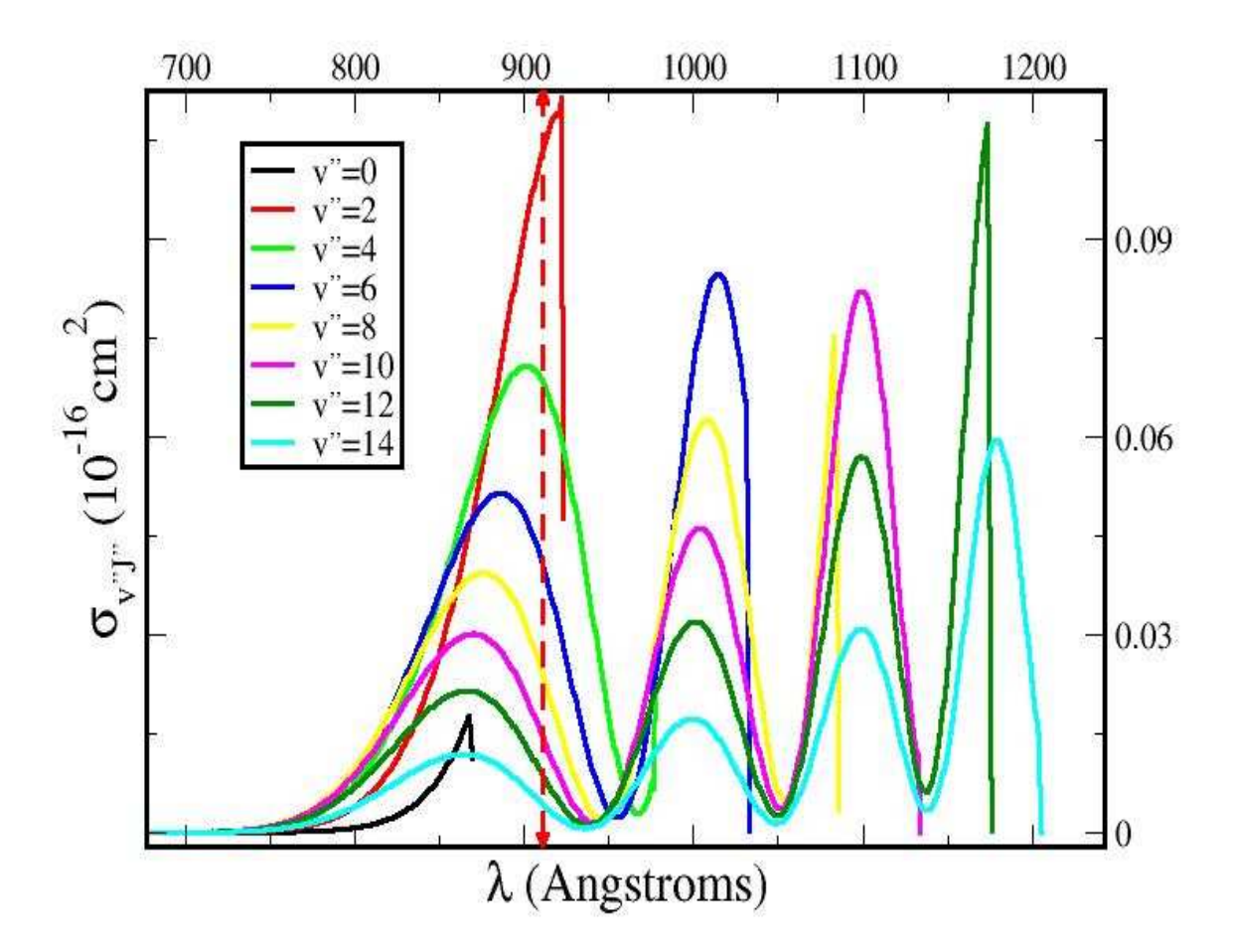


Figure 3.11. Partial cross sections for the Werner transition of HD from several vibrational levels corresponding to rotational quantum number J=9 of the ground electronic state.

Figures 3.12 and 3.13 compare our results with the calculations of Allison & Dalgarno (1969) for the v = 0, J = 0 HD cross sections as well as with those for H<sub>2</sub> (Gay et al., 2008).

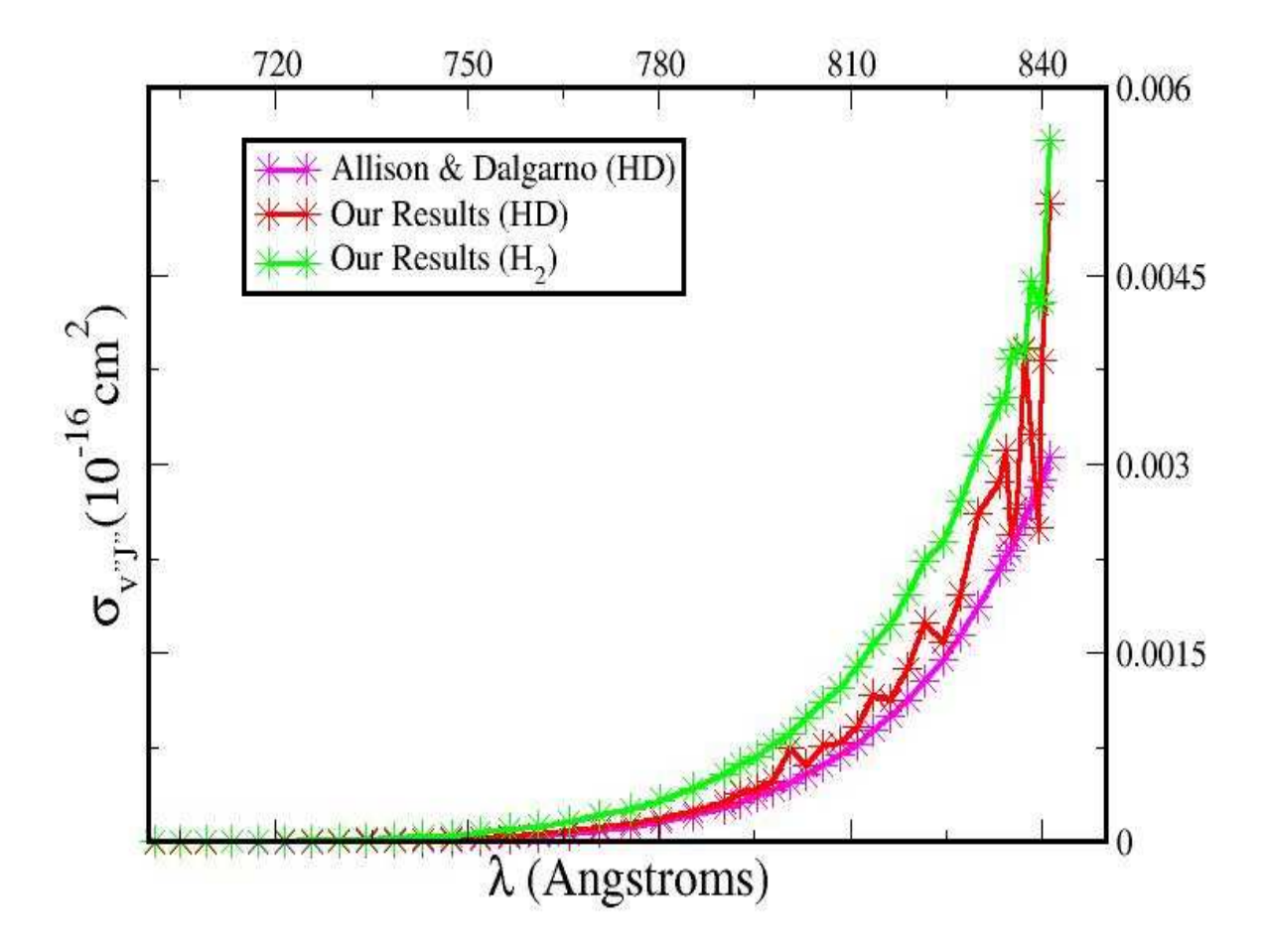


Figure 3.12. Partial cross sections for the Lyman transition from the v=0, J=0 rovibrational level of the ground state of HD and H<sub>2</sub>. Compares Gay et al. (2008) H<sub>2</sub> cross sections and Allison & Dalgarno (1969) HD cross sections with our results for HD.

As the plots show, our calculations of cross sections successfully reproduce the previous results obtained by Allison & Dalgarno (1969) for the v = 0, J = 0 rovibrational level of the ground state of HD (their cross sections have been computed only for the J = 0 states). The slight difference between the two data sets might reside in the improved potential curves and dipole transition moments used in the present work. Moreover, the difference between the HD and H<sub>2</sub> cross

sections is explained by their slightly different masses and thus rovibrational energies of their corresponding ground states.

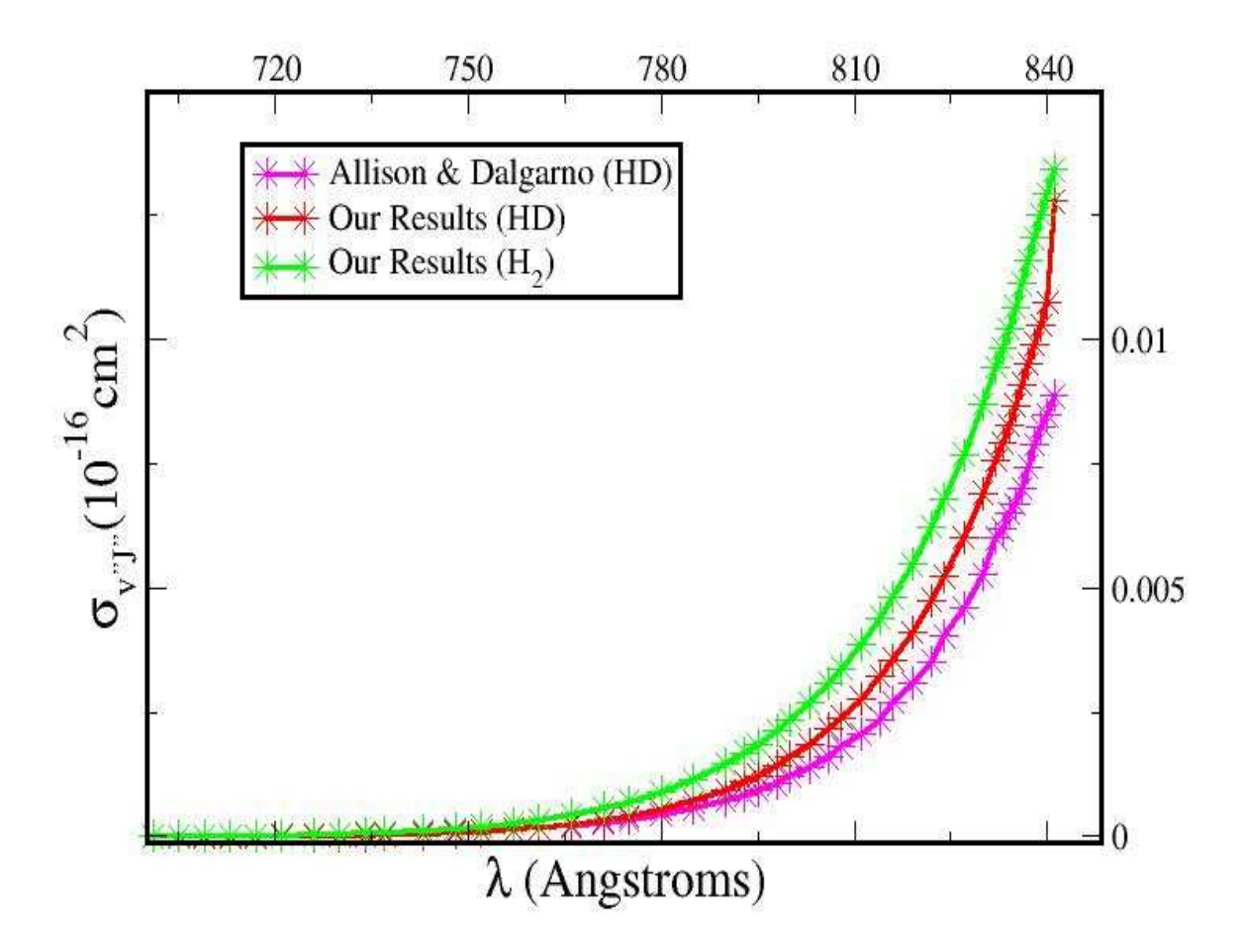


Figure 3.13. Partial cross sections for the Werner transition from the v = 0, J = 0 rovibrational level of the ground state of HD and H<sub>2</sub>. Compares Gay et al. (2008) H<sub>2</sub> cross sections and Allison & Dalgarno (1969) HD cross sections with our results for HD.

Figure 3.14 compares Lyman transition HD and  $H_2$  cross sections from rovibrational levels v = 0, J = 31, and v = 9, J = 0 of their ground electronic states, while Figure 3.15 does the same for the Werner transition. As expected, photodissociation thresholds for  $H_2$  cross sections are shifted to longer wavelengths relative to HD. This is consistent with the fact that the

rovibrational energy levels of the ground state of  $H_2$  are higher (due to its lighter mass) than their HD counterparts and it thus takes less energy to reach the continua of the upper states.

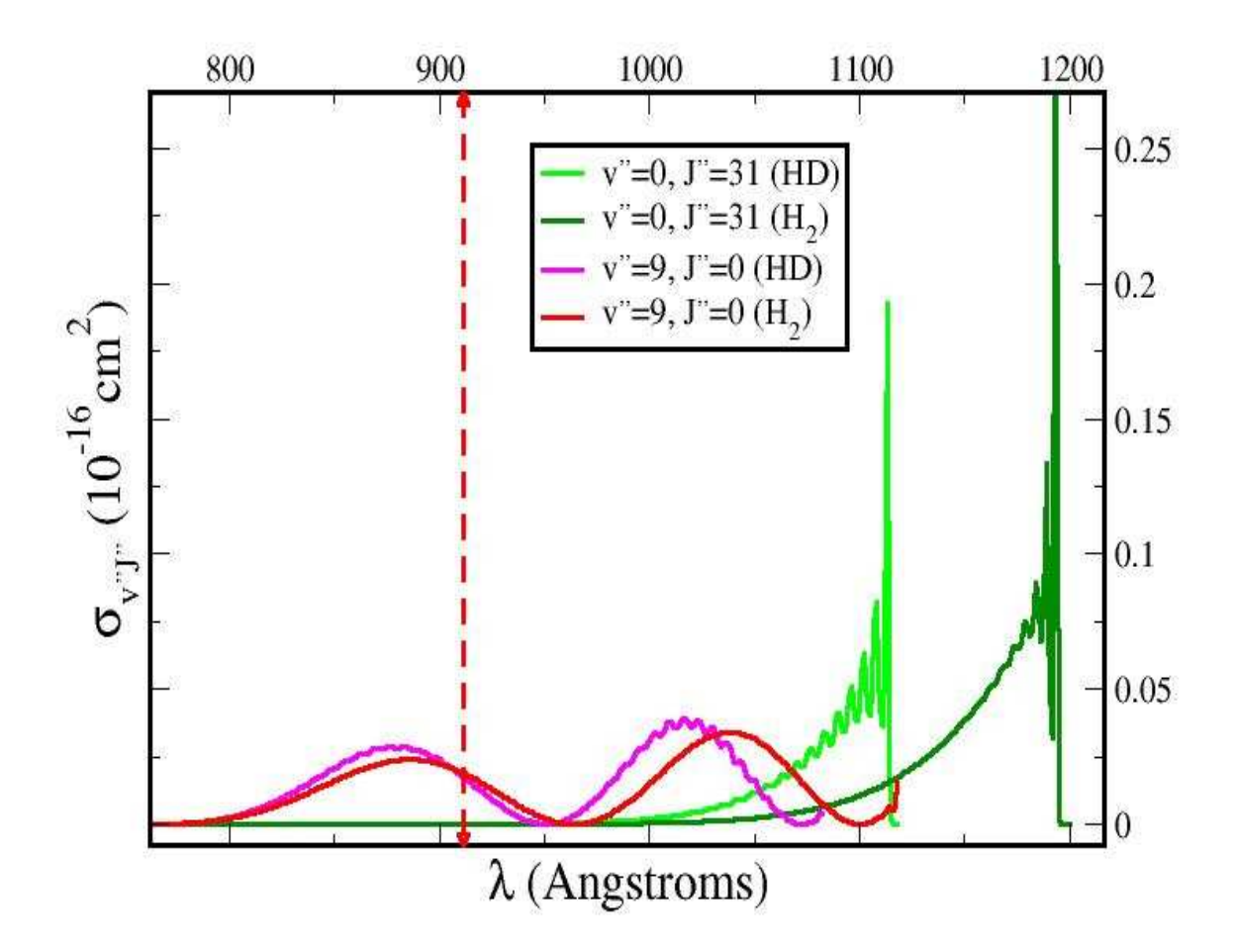


Figure 3.14. Lyman transition HD and H<sub>2</sub> (Gay et al., 2008) cross sections from the v = 0, J = 31 and v = 9, J = 0 rovibrational levels of their respective ground electronic states.

Figure 3.16 plots the cross sections for the Lyman as well as for the Werner transitions of HD and H<sub>2</sub> from the v = 9, J = 16 rovibrational level of their ground states. Aside from the shift in H<sub>2</sub> cross sections, Figure 3.16 also illustrates the difference between the two transitions from this particular level.

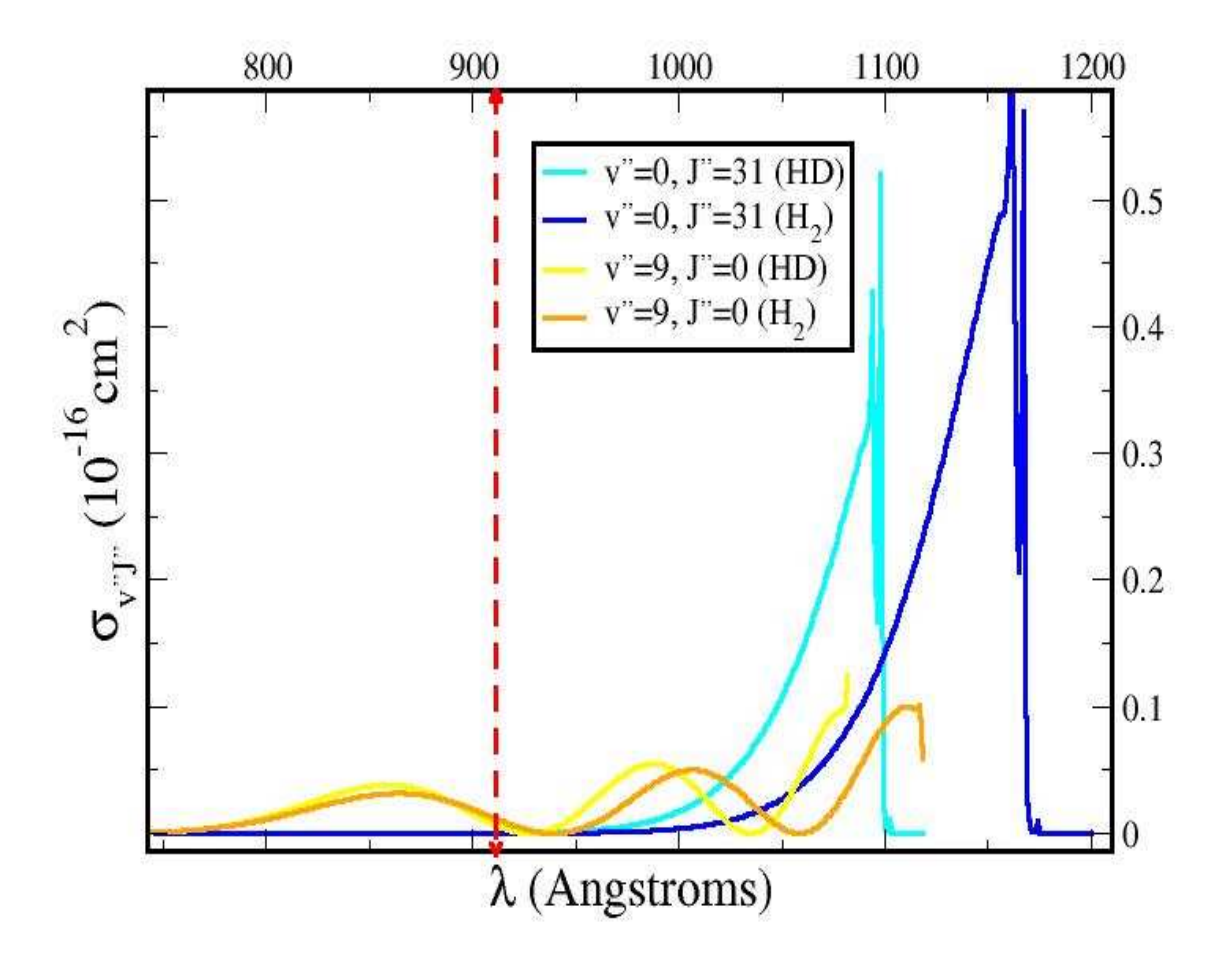


Figure 3.15. Werner transition HD and H<sub>2</sub> (Gay et al., 2008) cross sections from the v = 0, J = 31 and v = 9, J = 0 rovibrational levels of their respective ground electronic states.

The Werner  $(C \leftarrow X)$  cross sections appear to be significantly larger than their Lyman  $(B \leftarrow X)$  counterparts for both HD and H<sub>2</sub>. This is likely related to the fact that the B state is more bound than the C state, as they are, respectively,  $\Sigma$  and  $\Pi$  states, with the former corresponding to a much stronger covalent bond. Therefore a larger portion of the electronic transition probability goes to the continuum in the  $C \leftarrow X$  transition, than in the  $B \leftarrow X$  transition. This effect is evident from all of the Figures above: the Werner cross sections always peak higher and are on average greater than the Lyman cross sections for matching v and J combinations. The Lyman

transition cross sections also appear less smooth than the Werner cross sections, possibly due to a small barrier in the *B* state potential.

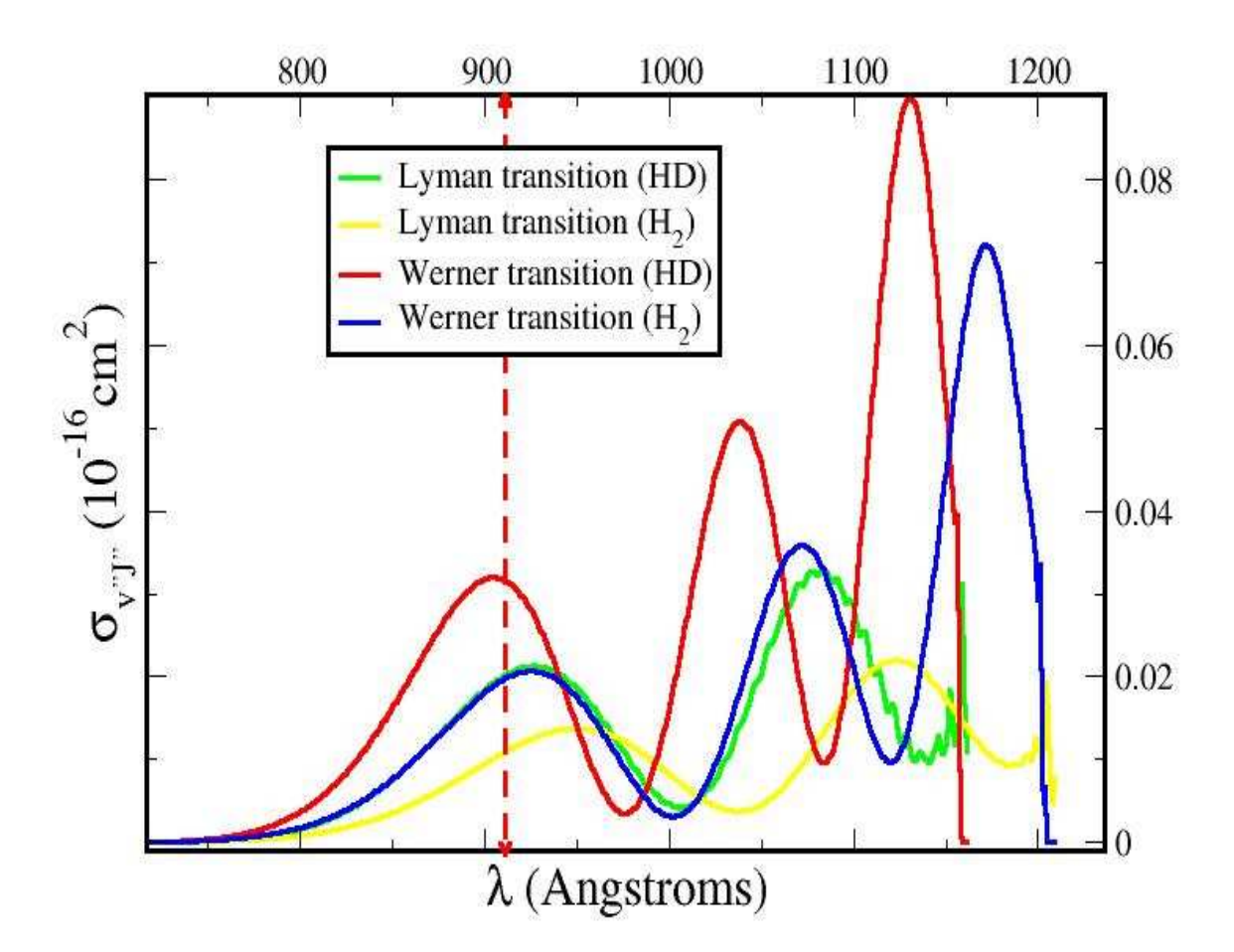


Figure 3.16. Lyman and Werner transition cross sections for HD and H<sub>2</sub> from the v = 9, J = 16 rovibrational level of their corresponding ground states.

#### Chapter 4

#### CONCLUSION AND FUTURE TOPICS

## 4.1 Summary

Rovibrational energies, totaling 400 levels, of the ground (X) state of HD have been calculated by a standard Numerov method. The energies, along with potential curves for the X, B, and C electronic states of HD as well as electric dipole transition moments between them, were used to calculate photodissociation cross sections corresponding to the Lyman ( $B \leftarrow X$ ) and Werner ( $C \leftarrow X$ ) transitions of HD, where B and C are, respectively, the first and second excited electronic states of the molecule. The potential energy curves had been previously computed by standard ab initio techniques such as solving the electronic eigenvalue equation for a number of internuclear distances R. In this work, the radial nuclear eigenvalue equation was solved, also by a Numerov method, for the vibrational and continuum wavefunctions which, along with the (previously computed) dipole transition moments, determine the cross sections as functions of photon energy. The cross sections were obtained from all 400 rovibrational levels of the ground electronic state and for a photon wavelength ranging from 100 Å to the dissociation threshold for each state.

Several patterns were observed in the cross sections. First, the thresholds shift to larger wavelengths with increasing v and J, namely the vibrational and rotational quantum numbers, as less energy is required to reach the continuum of the B or C state from a more excited rovibrational level of the X state. Cross sections for these particular channels are zero at wavelengths larger than the threshold and become very small for wavelengths shorter than approximately 700 Å, as either the photon energy is not sufficient to ignite the dissociation of the molecule or as transitions to other excited electronic states become significant, respectively.

Moreover, the cross sections exhibit nodes and antinodes at higher v, due mainly to the oscillating behavior of the vibrational and continuum wavefunctions. The cross sections were compared and found to be in agreement with previous results from Allison & Dalgarno (1969) for the v = 0, J = 0 rovibrational state (the only HD state for which cross sections have been previously calculated). They were further compared with previous cross section results for  $H_2$  (Gay et al., 2008), whose slightly lower mass results in higher rovibrational energy levels and thus photodissociation thresholds being shifted to longer wavelengths. Cross sections provide a direct and more accurate measure of the photodissociation processes for a particular molecule and ambient radiation field, as their computation requires no assumptions for the characteristics of a given astrophysical environment.

### 4.1 Future Work

The cross sections may be used to calculate HD photo-destruction rates for various astronomical environments as functions of temperature. Once photodissociation rates are obtained, they may be further used to determine abundances of HD in the given environments. HD is one of many molecules for which only limited cross section calculations currently exist (Allison & Dalgarno, 1969). Photodissociation data for many other molecules have been obtained through pre-computed, exponentially-attenuated fitted photo-rates, whose assumptions are typical of the interstellar medium and are likely to describe few other astrophysical environments. Thus computing cross sections for various transitions of astrophysically-relevant molecules and then integrating over the local radiation fields is necessary for accurate modeling of molecular abundances and overall physics of the environments of interest. Our current HD cross sections as well as future calculations for other species are scheduled to be implemented into Cloudy, a spectral simulation code designed to self-consistently determine the ionization and

excitation states of its components (Shaw, 2005). For the purpose of calculating HD photodissociation rates, cross sections through the Lyman and Werner transitions are generally sufficient. One might calculate cross sections corresponding to higher electronic transitions, but they are relatively insignificant. In particular, for environments typical of interstellar radiation, a majority of photons are removed at higher energies by ionization of atomic Hydrogen and are thus unavailable for dissociating the molecule.

The cross section data will be posted on the UGA Molecular Opacity Project website: www.physast.uga.edu/ugamop.

#### REFERENCES

Allison, A. C., & Dalgarno, A. 1969, At. Data, 1, 91.

Balakrishnan, A., Vallet, M., & Stoicheff, B. P. 1993, J. Mol. Spectrosc., 162, 168.

Cooley, J. W. 1961, Math. Computation, 15, 363.

Coursey, J. S., Schwab, D. J., & Dragoset, R. A. 2005, NIST Standard Reference Database 144, National Institute of Standards and Technology.

Draine, B. T. 1978, ApJS, 36, 595.

Dressler, K., & Wolniewicz, L. 1985, J. Chem. Phys., 82, 10.

Gay, C. D., Stancil, P. C., Shaw, G., & Ferland, G. J. 2008, in preparation.

Kirby, K. P., & Van Dishoeck, E. F. 1988, Adv. At. Mol. Phys., 25, 437.

Kolos, W., Szalewicz, K., & Monkhorst, H. J. 1986, J. Chem. Phys., 84, 3278-3283.

Kolos, W., & Wolniewicz, L. 1965, J. Chem. Phys., 43, 7.

Kolos, W., & Wolniewicz, L. 1968, J. Chem. Phys., 48, 3672.

Perry, J. B., 2005, Spectroscopically Accurate Calculated Properties of H<sub>2</sub>, Master Thesis, University of Georgia.

Schinke, R. 1993, Photodissociation Dynamics, Cambridge University Press.

Shaw, G., Ferland, G. J., Abel, N. P., Stancil, P. C., & Van Hoof, P. A. M. 2005, Astrophys. J., 624, 794.

Van Dishoeck, E. F. 1987, in IAU Symposium 120, Astrochemistry, ed. M. S. Vardya and S. P. Tarafdar (Dordrecht: Reidel), p. 51.

Wolniewicz, L. 1993, J. Chem. Phys., 99, 1851.

Wolniewicz, L. 1995, J. Chem. Phys., 103, 1792.

Appendix

# **Binding Energies of the Ground State of HD**

v	J	Energy (a.u.)	Energy (cm <sup>-1</sup> )
0	0	0.16588251E+00	0.36406998E+05
0	1	0.16547598E+00	0.36317774E+05
0	2	0.16466570E+00	0.36139939E+05
0	3	0.16345722E+00	0.35874708E+05
0	4	0.16185867E+00	0.35523868E+05
0	5	0.15988061E+00	0.35089734E+05
0	6	0.15753578E+00	0.34575102E+05
0	7	0.15483883E+00	0.33983189E+05
0	8	0.15180605E+00	0.33317571E+05
0	9	0.14845506E+00	0.32582115E+05
0	10	0.14480453E+00	0.31780915E+05
0	11	0.14087385E+00	0.30918232E+05
0	12	0.13668292E+00	0.29998429E+05
0	13	0.13225186E+00	0.29025924E+05
0	14	0.12760082E+00	0.28005140E+05
0	15	0.12274979E+00	0.26940461E+05
0	16	0.11771842E+00	0.25836202E+05
0	17	0.11252592E+00	0.24696580E+05
0	18	0.10719095E+00	0.23525691E+05
0	19	0.10173155E+00	0.22327491E+05
0	20	0.96165070E-01	0.21105790E+05
0	21	0.90508158E-01	0.19864242E+05
0	22	0.84776728E-01	0.18606339E+05
0	23	0.78985973E-01	0.17335415E+05
0	24	0.73150369E-01	0.16054648E+05
0	25	0.67283708E-01	0.14767065E+05
0	26	0.61399122E-01	0.13475548E+05
0	27	0.55509135E-01	0.12182845E+05
0	28	0.49625710E-01	0.10891583E+05
0	29	0.43760308E-01	0.96042760E+04
0	30	0.37923954E-01	0.83233446E+04
0	31	0.32127319E-01	0.70511304E+04
0	32	0.26361503E-01	0.57856803E+04
0	33	0.20675208E-01	0.45376829E+04
0	34	0.15059533E-01	0.33051849E+04
0	35	0.95248099E-02	0.20904538E+04

0	36	0.40817018E-02	0.89582987E+03
1	0	0.14933174E+00	0.32774524E+05
1	1	0.14894277E+00	0.32689155E+05
1	2	0.14816755E+00	0.32519014E+05
1	3	0.14701145E+00	0.32265279E+05
1	4	0.14548237E+00	0.31929685E+05
1	5	0.14359054E+00	0.31514477E+05
1	6	0.14134833E+00	0.31022368E+05
1	7	0.13876994E+00	0.30456476E+05
1	8	0.13587114E+00	0.29820265E+05
1	9	0.13266901E+00	0.29117478E+05
1	10	0.12918161E+00	0.28352081E+05
1	11	0.12542770E+00	0.27528194E+05
1	12	0.12142653E+00	0.26650040E+05
1	13	0.11719757E+00	0.25721890E+05
1	14	0.11276031E+00	0.24748023E+05
1	15	0.10813407E+00	0.23732682E+05
1	16	0.10333791E+00	0.22680046E+05
1	17	0.98390422E-01	0.21594198E+05
1	18	0.93309724E-01	0.20479114E+05
1	19	0.88113337E-01	0.19338639E+05
1	20	0.82818162E-01	0.18176483E+05
1	21	0.77440449E-01	0.16996211E+05
1	22	0.71995789E-01	0.15801247E+05
1	23	0.66499125E-01	0.14594869E+05
1	24	0.60964769E-01	0.13380218E+05
1	25	0.55406434E-01	0.12160305E+05
1	26	0.49837285E-01	0.10938018E+05
1	27	0.44269987E-01	0.97161377E+04
1	28	0.38716781E-01	0.84973500E+04
1	29	0.33189558E-01	0.72842649E+04
1	30	0.27699960E-01	0.60794377E+04
1	31	0.22259502E-01	0.48853952E+04
1	32	0.16879712E-01	0.37046679E+04
1	33	0.10879712E-01 0.11572328E-01	0.25398320E+04
1	34	0.63312955E-02	0.13895585E+04
1	35	0.12063513E-02	0.26476348E+03
2	0	0.12003313E-02 0.13358950E+00	0.29319501E+05
2	1	0.13338930E+00 0.13321774E+00	0.29319301E+03 0.29237910E+05
2	2	0.13321774E+00 0.13247687E+00	0.29237910E+03 0.29075308E+05
2	3	0.13137211E+00	0.28832840E+05
2	4	0.12991111E+00	0.28512190E+05
2	5	0.12810383E+00	0.28115538E+05
2	6	0.12596226E+00	0.27645517E+05
2	7	0.12350017E+00	0.27105151E+05

2	Q	0.12072207E±00	0.26497799E+05
2	8	0.12073287E+00	
		0.11767691E+00	0.25827092E+05
2	10	0.11434978E+00	0.25096871E+05
2	11	0.11076967E+00	0.24311130E+05
2	12	0.10695524E+00	0.23473959E+05
2	13	0.10292535E+00	0.22589499E+05
2	14	0.98698886E-01	0.21661898E+05
2	15	0.94294616E-01	0.20695273E+05
2	16	0.89731024E-01	0.19693681E+05
2	17	0.85026211E-01	0.18661094E+05
2	18	0.80197814E-01	0.17601383E+05
2	19	0.75262944E-01	0.16518304E+05
2	20	0.70238150E-01	0.15415490E+05
2	21	0.65139407E-01	0.14296445E+05
2	22	0.59982109E-01	0.13164549E+05
2	23	0.54781094E-01	0.12023059E+05
2	24	0.49550673E-01	0.10875114E+05
2	25	0.44304679E-01	0.97237517E+04
2	26	0.39056533E-01	0.85719169E+04
2	27	0.33819321E-01	0.74224819E+04
2	28	0.28605896E-01	0.62782676E+04
2	29	0.23429008E-01	0.51420721E+04
2	30	0.18301459E-01	0.40167054E+04
2	31	0.13236325E-01	0.29050372E+04
2	32	0.82472425E-02	0.18100602E+04
2	33	0.33488264E-02	0.73498234E+03
3	0	0.11863990E+00	0.26038444E+05
3	1	0.11828509E+00	0.25960574E+05
3	2	0.11757805E+00	0.25805396E+05
3	3	0.11652385E+00	0.25574025E+05
3	4	0.11512993E+00	0.25268096E+05
3	5	0.11340597E+00	0.24889730E+05
3	6	0.11136360E+00	0.24441481E+05
3	7	0.10901621E+00	0.23926289E+05
3	8	0.10637866E+00	0.23347413E+05
3	9	0.10346701E+00	0.22708380E+05
3	10	0.10029824E+00	0.22012916E+05
3	11	0.96890027E-01	0.21264900E+05
3	12	0.93260466E-01	0.20468303E+05
3	13	0.89427886E-01	0.19627150E+05
3	14	0.85410661E-01	0.18745471E+05
3	15	0.81227049E-01	0.17827274E+05
3	16	0.76895071E-01	0.17827274E+03 0.16876515E+05
3	17	0.72432410E-01	0.15897074E+05
3	18	0.67856340E-01	0.13897074E+03 0.14892743E+05
3	10	U.0763034UE-UI	U.14894/43E#US

3	19	0.63183673E-01	0.13867211E+05
3	20	0.58430742E-01	0.12824064E+05
3	21	0.53613388E-01	0.11766777E+05
3	22	0.48746981E-01	0.10698724E+05
3	23	0.43846451E-01	0.96231822E+04
3	24	0.38926343E-01	0.85433435E+04
3	25	0.34000892E-01	0.74623322E+04
3	26	0.29084122E-01	0.63832259E+04
3	27	0.24189972E-01	0.53090845E+04
3	28	0.19332473E-01	0.42429868E+04
3	29	0.14525967E-01	0.31880809E+04
3	30	0.97854290E-02	0.21476531E+04
3	31	0.51269205E-02	0.11252288E+04
3	32	0.56829478E-03	0.12472627E+03
4	0	0.10447168E+00	0.22928880E+05
4	1	0.10413366E+00	0.22854694E+05
4	2	0.10346012E+00	0.22706869E+05
4	3	0.10346012E+00 0.10245600E+00	0.22486490E+05
4	4	0.10243000E+00	0.22195148E+05
4	5	0.99487159E-01	0.21834904E+05
4	6	0.97543159E-01	0.21408246E+05
4	7	0.95309567E-01	0.20918029E+05
4	8	0.92800833E-01	0.20367426E+05
4	9	0.92800833E-01 0.90032573E-01	0.19759863E+05
4	10	0.90032373E-01 0.87021313E-01	0.19739803E+03 0.19098968E+05
4	11	0.83784240E-01	0.19098908E+05
4	12	0.80338982E-01	0.17632366E+05
4	13	0.76703402E-01	0.17632360E+05
4	14	0.70703402E-01 0.72895431E-01	0.15998696E+05
4	15	0.68932919E-01	0.15129025E+05
4		0.64833525E-01	0.13129023E+03 0.14229312E+05
	16		
4	17	0.60614626E-01	0.13303371E+05
4	18	0.56293264E-01	0.12354942E+05
4	19	0.51886102E-01	0.11387682E+05
4	20	0.47409424E-01	0.10405164E+05
4	21	0.42879142E-01	0.94108826E+04
4	22	0.38310836E-01	0.84082555E+04
4	23	0.33719817E-01	0.74006433E+04
4	24	0.29121216E-01	0.63913672E+04
4	25	0.24530111E-01	0.53837364E+04
4	26	0.19961700E-01	0.43810862E+04
4	27	0.15431530E-01	0.33868289E+04
4	28	0.10955829E-01	0.24045262E+04
4	29	0.65519891E-02	0.14379952E+04
4	30	0.22393075E-02	0.49147111E+03

5	Λ	0.01070527E.01	0.10090425E±05
5	0	0.91078537E-01 0.90757248E-01	0.19989425E+05
	1	***************************************	0.19918911E+05
5	2	0.90117104E-01	0.19778415E+05
5	3	0.89162914E-01	0.19568995E+05
5	4	0.87901743E-01	0.19292200E+05
5	5	0.86342743E-01	0.18950039E+05
5	6	0.84496951E-01	0.18544934E+05
5	7	0.82377048E-01	0.18079670E+05
5	8	0.79997115E-01	0.17557335E+05
5	9	0.77372375E-01	0.16981271E+05
5	10	0.74518946E-01	0.16355016E+05
5	11	0.71453605E-01	0.15682251E+05
5	12	0.68193579E-01	0.14966758E+05
5	13	0.64756351E-01	0.14212374E+05
5	14	0.61159508E-01	0.13422958E+05
5	15	0.57420603E-01	0.12602364E+05
5	16	0.53557061E-01	0.11754414E+05
5	17	0.49586102E-01	0.10882890E+05
5	18	0.45524705E-01	0.99915164E+04
5	19	0.41389586E-01	0.90839629E+04
5	20	0.37197220E-01	0.81638449E+04
5	21	0.32963877E-01	0.72347336E+04
5	22	0.28705704E-01	0.63001729E+04
5	23	0.24438839E-01	0.53637045E+04
5	24	0.20179576E-01	0.44289044E+04
5	25	0.15944596E-01	0.34994338E+04
5	26	0.11751303E-01	0.25791125E+04
5	27	0.76183172E-02	0.16720271E+04
5	28	0.35662411E-02	0.78269934E+03
6	0	0.78459635E-01	0.17219897E+05
6	1	0.78155140E-01	0.17153068E+05
6	2	0.77548527E-01	0.17019932E+05
6	3	0.76644487E-01	0.16821518E+05
6	4	0.75449919E-01	0.16559341E+05
6	5	0.73973756E-01	0.16235360E+05
6	6	0.72226774E-01	0.15851942E+05
6	7	0.70221360E-01	0.15411805E+05
6	8	0.67971273E-01	0.14917968E+05
6	9	0.65491399E-01	0.14373699E+05
6	10	0.62797515E-01	0.13782459E+05
6	11	0.59906066E-01	0.13147860E+05
6	12	0.56833970E-01	0.12473613E+05
6	13	0.53598437E-01	0.11763496E+05
6	14	0.50216832E-01	0.11021319E+05
6	15	0.46706556E-01	0.10250903E+05
U	13	0.40/00330E-01	0.10230303E+03

6	16	0.43084970E-01	0.94560565E+04
6	17	0.39369336E-01	0.86405692E+04
6	18	0.35576808E-01	0.78082057E+04
6	19	0.31724447E-01	0.69627104E+04
6	20	0.27829275E-01	0.61078189E+04
6	21	0.23908370E-01	0.52472799E+04
6	22	0.19979026E-01	0.43848887E+04
6	23	0.16058970E-01	0.35245360E+04
6	24	0.12166696E-01	0.26702808E+04
6	25	0.83219610E-02	0.18264591E+04
6	26	0.45465568E-02	0.99785373E+03
6	27	0.86561205E-03	0.18997986E+03
7	0	0.66620287E-01	0.14621461E+05
7	1	0.66332795E-01	0.14558364E+05
7	2	0.65760136E-01	0.14432679E+05
7	3	0.64906901E-01	0.14245416E+05
7	4	0.63779841E-01	0.13998055E+05
7	5	0.62387701E-01	0.13692516E+05
7	6	0.60741034E-01	0.13331114E+05
7	7	0.58851982E-01	0.12916515E+05
7	8	0.56734040E-01	0.12451681E+05
7	9	0.54401829E-01	0.11939820E+05
7	10	0.51870868E-01	0.11384338E+05
7	11	0.49157371E-01	0.10788794E+05
7	12	0.49137371E-01 0.46278062E-01	0.10788794E+03
7	13	0.43250016E-01	0.10130839E+03 0.94922800E+04
7	14	0.40090543E-01	0.87988559E+04
7	15	0.40090343E-01 0.36817089E-01	0.80804158E+04
7	16	0.33447183E-01	0.73408071E+04
7	17	0.39998424E-01	0.65838920E+04
7		0.29998424E-01 0.26488498E-01	0.58135526E+04
	18	0,-0.00.70-0-	
7	19	0.22935260E-01	0.50337070E+04
7	20	0.19356858E-01	0.42483386E+04
7	21	0.15771946E-01	0.34615415E+04
7	22	0.12200004E-01	0.26775910E+04
7	23	0.86618249E-02	0.19010506E+04
7	24	0.51802897E-02	0.11369420E+04
7	25	0.17816718E-02	0.39103171E+03
8	0	0.55572867E-01	0.12196833E+05
8	1	0.55302759E-01	0.12137551E+05
8	2	0.54764824E-01	0.12019488E+05
8	3	0.53963572E-01	0.11843633E+05
8	4	0.52905628E-01	0.11611442E+05
8	5	0.51599591E-01	0.11324800E+05
8	6	0.50055838E-01	0.10985985E+05

8	7	0.48286325E-01	0.10597622E+05
8	8	0.46304359E-01	0.10397622E+03
8	9	0.44124388E-01	0.96841824E+04
8	10	0.44724388E-01 0.41761784E-01	0.91656509E+04
8	11	0.39232661E-01	0.86105727E+04
8	12	0.36553709E-01	0.80226107E+04
8	13	0.33742062E-01	0.74055257E+04
8	14	0.30815205E-01	0.67631548E+04
8	15	0.27790914E-01	0.60993997E+04
8	16	0.24687247E-01	0.54182236E+04
8	17	0.21522583E-01	0.47236602E+04
8	18	0.18315726E-01	0.40198366E+04
8	19	0.15086089E-01	0.33110135E+04
8	20	0.11853998E-01	0.26016514E+04
8	21	0.86411603E-02	0.18965152E+04
8	22	0.54714402E-02	0.12008422E+04
8	23	0.23721596E-02	0.52062878E+03
9	0	0.45338051E-01	0.99505507E+04
9	1	0.45085918E-01	0.98952139E+04
9	2	0.44583903E-01	0.97850342E+04
9	3	0.43836450E-01	0.96209874E+04
9	4	0.42850103E-01	0.94045091E+04
9	5	0.41633352E-01	0.91374634E+04
9	6	0.40196468E-01	0.88221038E+04
9	7	0.38551299E-01	0.84610308E+04
9	8	0.36711065E-01	0.80571464E+04
9	9	0.34690164E-01	0.76136098E+04
9	10	0.32503974E-01	0.71337967E+04
9	11	0.30168695E-01	0.66212622E+04
9	12	0.27701211E-01	0.60797122E+04
9	13	0.25118996E-01	0.55129817E+04
9	14	0.22440065E-01	0.49250243E+04
9	15	0.19682973E-01	0.43199126E+04
9	16	0.16866887E-01	0.43199120E+04 0.37018533E+04
9	17	0.14011741E-01	0.30752213E+04
9	18	0.14011741E-01 0.11138508E-01	0.24446196E+04
9	19	0.82696566E-02	0.24446196E+04 0.18149796E+04
		0.82696366E-02 0.54299082E-02	
9	20		0.11917269E+04
	21	0.26475460E-02	0.58106909E+03
10	0	0.35946500E-01	0.78893438E+04
10	1	0.35713198E-01	0.78381399E+04
10	2	0.35248826E-01	0.77362221E+04
10	3	0.34557800E-01	0.75845593E+04
10	4	0.33646620E-01	0.73845786E+04
10	5	0.32523743E-01	0.71381355E+04

10	6	0.31199412E-01	0.68474785E+04
10	7	0.29685481E-01	0.65152090E+04
10	8	0.27995225E-01	0.61442409E+04
10	9	0.26143167E-01	0.57377612E+04
10	10	0.24144914E-01	0.52991953E+04
10	11	0.22017026E-01	0.48321781E+04
10	12	0.19776936E-01	0.43405351E+04
10	13	0.17442905E-01	0.38282747E+04
10	14	0.15034062E-01	0.32995947E+04
10	15	0.12570519E-01	0.27589097E+04
10	16	0.10073622E-01	0.22109042E+04
10	17	0.75663799E-02	0.16606282E+04
10	18	0.50742099E-02	0.11136602E+04
10	19	0.26262651E-02	0.57639848E+03
10	20	0.25800530E-03	0.56625610E+02
11	0	0.27441117E-01	0.60226281E+04
11	1	0.27227839E-01	0.59758192E+04
11	2	0.26803521E-01	0.58826921E+04
11	3	0.26172589E-01	0.57442185E+04
11	4	0.25341572E-01	0.55618314E+04
11	5	0.24318981E-01	0.53373987E+04
11	6	0.23115162E-01	0.50731910E+04
11	7	0.21742136E-01	0.47718466E+04
11	8	0.20213443E-01	0.44363373E+04
11	9	0.18543999E-01	0.40699368E+04
11	10	0.16749984E-01	0.36761960E+04
11	11	0.14848771E-01	0.32589280E+04
11	12	0.12858925E-01	0.28222074E+04
11	13	0.10800290E-01	0.23703894E+04
11	14	0.86942031E-02	0.19081568E+04
11	15	0.65639066E-02	0.14406108E+04
11	16	0.44352944E-02	0.97343446E+03
11	17	0.23382812E-02	0.51319334E+03
11	18	0.30956011E-03	0.67940580E+02
12	0	0.19880111E-01	0.43631793E+04
12	1	0.19688503E-01	0.43211263E+04
12	2	0.19307559E-01	0.42375188E+04
12	3	0.19307337E-01 0.18741782E-01	0.41133451E+04
12	4	0.17997830E-01	0.39500665E+04
12	5	0.17084412E-01	0.37495946E+04
12	6	0.16012169E-01	0.35142644E+04
12	7	0.14793546E-01	0.32468076E+04
12	8	0.13442685E-01	0.29503279E+04
12	9	0.13442083E-01 0.11975343E-01	0.26282836E+04
12	10	0.11973343E-01 0.10408868E-01	0.20282830E+04 0.22844821E+04
12	10	U.1U4U8808E-U1	U.22044021E±U4

12	11	0.87622578E-02	0.19230930E+04
12	12	0.70563526E-02	0.15486902E+04
12	13	0.53142329E-02	0.11663391E+04
12	14	0.35619845E-02	0.78176513E+03
12	15	0.18301732E-02	0.40167654E+03
12	16	0.15698832E-03	0.34454948E+02
13	0	0.13341187E-01	0.29280516E+04
13	1	0.13173515E-01	0.28912519E+04
13	2	0.12840527E-01	0.28181696E+04
13	3	0.12346906E-01	0.27098323E+04
13	4	0.11699601E-01	0.25677652E+04
13	5	0.10907753E-01	0.23939747E+04
13	6	0.99826222E-02	0.21909320E+04
13	7	0.89375233E-02	0.19615594E+04
13	8	0.77878079E-02	0.17092260E+04
13	9	0.65509222E-02	0.14377610E+04
13	10	0.52465944E-02	0.11514942E+04
13	11	0.38972492E-02	0.85534721E+03
13	12	0.25288392E-02	0.55501597E+03
13	13	0.11725553E-02	0.25734611E+03
14	0	0.79273875E-02	0.17398602E+04
14	1	0.77868237E-02	0.17090100E+04
14	2	0.75082234E-02	0.16478643E+04
14	3	0.70966265E-02	0.15575293E+04
14	4	0.65595635E-02	0.14396576E+04
14	5	0.59070423E-02	0.12964457E+04
14	6	0.51515657E-02	0.11306378E+04
14	7	0.43082224E-02	0.94554540E+03
14	8	0.33949151E-02	0.74509762E+03
14	9	0.24328493E-02	0.53394863E+03
14	10	0.14475600E-02	0.31770265E+03
14	11	0.47123164E-03	0.10342338E+03
15	0	0.37753216E-02	0.82858721E+03
15	1	0.36664742E-02	0.80469797E+03
15	2	0.34516511E-02	0.75754975E+03
15	3	0.31366228E-02	0.68840903E+03
15	4	0.27301305E-02	0.59919429E+03
15	5	0.22440461E-02	0.49251112E+03
15	6	0.16937082E-02	0.37172592E+03
15	7	0.10986327E-02	0.24112198E+03
15	8	0.48414516E-03	0.10625756E+03
16	0	0.10660358E-02	0.23396778E+03
16	1	0.99620028E-03	0.21864066E+03
16	2	0.86024343E-03	0.18880158E+03
16	3	0.66581864E-03	0.14613028E+03

16	4	0.42513345E-03	0.93305995E+02
16	5	0.15661288E-03	0.34372548E+02
17	0	0.15993088E-04	0.35100767E+01
17	1	0.15430933E-05	0.33866977E+00